Towards a multi-epitope cell imaging technique assisted by metal-chelating polymers and SEM-EDS

By

Rudolf Dreyer

Thesis presented in fulfilment of the requirements for the degree of Masters of Science (Polymer Science)

at

Stellenbosch University

Supervisor: Prof. Bert Klumperman
Co-supervisor: Dr. Rueben Pfukwa

Department of Chemistry and Polymer Science

Faculty of Science

March 2018

Declaration

By submitting this thesis/dissertation electronically, I declare that the entirety of the work contained therein is my own, original work, that I am the sole author thereof (save to the extent explicitly otherwise stated), that reproduction and publication thereof by Stellenbosch University will not infringe any third-party rights and that I have not previously in its entirety or in part submitted it for obtaining any qualification

Rudolf Dreyer

Stellenbosch, 2017

Abstract

This thesis reports the design, synthesis and characterization of a novel trithiocarbonate chain transfer agent for reversible addition-fragmentation chain-transfer (RAFT) polymerization. The RAFT agent is designed with benzylguanine (BG) functionality built into the R-group. The rationale behind the RAFT agent design is to develop a facile route to the synthesis of polymers with α-BG functionality to be used as labels for SNAP-tag – a modified version of the hAGT enzyme with the ability to bind various BG-modified substrates.

The RAFT agent with BG functionality was successfully synthesized by the copper(I)-assisted azide-alkyne cycloaddition reaction of but-3-yn-2-yl carbonotrithioate and an O^6-(*p*-azidobenzyl)guanine derivative which we developed. The RAFT agent was used in the synthesis of poly(*tert*-butyl acrylate) (P*t*BA) showing good control and a low dispersity, and we were able to confirm the α-BG end-functionality of the polymer.

The synthesis of α-BG-functional P*t*BA was followed by a series of side-chain modifications, whilst retaining the α-BG chain-end. The first step was the deprotection of the butyl ester group to form poly(acrylic acid) (PAA), followed by a coupling reaction with *t*-BOC-ethylenediamine and the subsequent deprotection of the BOC groups to yield an amine-functional polymer. The final step was the attachment of a DTPA ligand to each repeat unit to form α-BG functional poly(DTPA) as a polymer easily capable of metal-chelation. Finally, we show that ω-chain-end modification of the polymer can be achieved by aminolysis of the ω-trithiocarbonate end-group followed by a thiol-Michael addition click reaction of a maleimide functional fluorescent dye, without affecting the α-BG chain-end.

The thesis reports the successful synthesis of a novel BG-functional RAFT agent, followed by preliminary investigations towards the development of α-BG-functional and ω-fluorescently labelled metal-chelating polymers (MCPs) which we aim to use in the development of a high resolution, spatial cell imaging technique assisted by SEM-EDS.

Opsomming

Hierdie tesis rapporteer die ontwerp, sintese en karakterisering van 'n nuwe trithiocarbonate ketting oordrag agent vir omkeerbare byvoeging-fragmentasie ketting-oordrag (RAFT) polimerisasie. Die RAFT agent is ontwerp met benzylguanine (BG) funksionaliteit by die R-groep ingebou. Die rasionaal agter die ontwerp is die ontwikkeling van ‘n eenvoudige roete tot die sintese van polimere met α-BG funksionaliteit as merkers vir SNAP-tag – 'n gewysigde weergawe van die hAGT ensiem met die vermoë om te bind met BG-gemodifiseerde molekules.

Die RAFT agent met BG funksionaliteit was suksesvol gesintetiseer deur die koper (I) -geassiseerde azide-alkyne sikloaddisie reaksie van but-3-yn-2-yl carbonotrithioate en 'n O^6-(p-azidobenzyl) guanine afgeleide wat ons ontwikkel het. Die RAFT agent was gebruik in die sintese van poly(*tert*-butyl acrylate) (P*t*BA) en toon goeie beheer en 'n lae ketinglengte verspreiding. Ons het die teenwoordigheid van die α-BG eindgroep van die polimeer bevestig.

Die sintese van α-BG-funksionele PtBA is gevolg deur 'n reeks kant-ketting modifikasies, met focus op die behoud van die α-BG eindgroep. Die eerste stap was die hidroliese van die butiel ester groep om poly(acrylic acid) (PAA) te vorm. Dit was gevolg deur 'n koppeling reaksie met *t*-BOC-ethylenediamine en die daaropvolgende verwydering van die BOC groepe om 'n amien-funksionele polimeer te vorm. Die finale stap was die aanheging van 'n DTPA ligand op elke herhaaleenheid om α-BG funksionele poly(DTPA) te vorm as 'n polimeer wat maklik met ‘n verskeidenheid metale kan bind. Hierna wys ons dat modifikasies van die ω-ketting-einde van die polimeer bereikbaar is deur aminoliese van die ω-trithiocarbonate einde-groep gevolg deur 'n thiol-Michael-byvoeging klik reaksie van 'n maleimide funksionele fluoresserende molekule, sonder om die α-BG ketting-einde te affekteer.

In opsomming rapporteer hierdie tesis die suksesvolle sintese van 'n BG-funksionele RAFT agent, gevolg deur voorlopige ondersoeke na die ontwikkeling van α-BG-funksionele en ω-fluoresserende metaal-chelaterende polimere (MCPs). Ons mik om hierdie te gebruik in die ontwikkeling van 'n hoë resolusie, ruimtelike cell imaging tegniek gehelp deur SEM-EDS.

Acknowledgements

To my supervisor, Prof. Klumperman, I would like to thank you for your advice and guidance throughout this project. Your vision and expertise are admirable, and it is a tremendous privilege to be a part of your research group. I wish to thank the NRF for financial assistance.

To my co-supervisor, Dr. Rueben Pfukwa, thank you for pushing me and somehow managing to get the best out of me. Your knowledge, continuous presence, and guidance have been tremendously helpful.

To Dr. Waled Hadasha, your patience and assistance have been invaluable. To Ingrid Heyns and Siyasanga Mbizana, thank you for all the assistance and advice, constantly pointing me in the right direction, and helping to make the long hours of writing a pleasure. To Janus Barnard, thank you for keeping me sane. To Chandré Smit and Nelmari Harmzen, thank you also for making the work environment fun.

To Elsa Malherbe and Dr. Jaco Brand, thank you for always going out of your way to help with NMR spectroscopic analysis. Thank you to Calvin Maart and Jim Motshweni for all your assistance. I also wish to thank Aneli Fourie, Erinda Cooper and Deon Koen for their contributions.

To past and present members of the Free Radical group, especially Rueben, Waled, Elrika, Anna, Lisa, Elaine, Shane, Justin, Nusrat, Feziwe, captain Simba, Benni, Luca, Welmarie, Ingrid, Nelmari, Chandré, Priscilla and Siya – thank you. Your friendships are appreciated and each of you have played a role in my development as a researcher. It has been a pleasure to work with you.

To my friends and family, thank you for supporting, looking after, and always believing in me. I am deeply indebted to you.

Table of contents

List of abbreviations

BG	Benzylguanine
BOC	*Tert*-butyloxycarbonyl
COSY	Homonuclear correlation spectroscopy
CTA	Chain transfer agent
CuAAC	CuI-catalyzed azide alkyne cycloaddition
DIPEA	Diisopropylethylamine
DMAP	4-Dimethylaminopyridine
DMF	Dimethylformamide
DMSO	Dimethyl sulfoxide
DMTMM	4-(4,6-Dimethoxy-1,3,5-triazin-2-yl)-4-methylmopholinium chloride
DNA	Deoxyribonucleid acid
DOTA	1,4,7,10-Tetraazocyclodecan-1,4,7,10-tetraacetic acid
DP	Degree of polymerization
DTP	2,2'-Dithiopyridine
DTPA	Diethylenetriaminepentaacetic acid
EDS	Energy-dispersive X-ray spectroscopy
FTIR	Fourier-transform infrared spectroscopy
gHMBC	Gradient heteronuclear multiple bond correlation
gHSQC	Gradient heteronuclear single quantum coherence
hAGT	Mutant of the human DNA repair enzyme
ICP-TOF-MS	Inductively coupled plasma time-of-flight mass spectrometry
ITC	Isothermal titration calorimetry
MCP	Metal-chelating polymer
Me6TREN	Tris[2-(dimethylamino)ethyl]amine
MRI	Magnetic resonance imaging
NMR	Nuclear magnetic resonance
PAA	Poly(acrylic acid)
PMDETA	*N,N,N',N'',N''*-Pentamethyldiethylenetriamine

P*t*BA	Poly(*tert*-butyl acrylate)
RAFT	Reversible addition-fragmentation chain-transfer
RDRP	Reversible deactivation radical polymerization
SEC	Size exclusion chromatography
SEM	Scanning electron microspocy
TCEP	Tris(2-carboxyethyl)phosphine
TFA	Trifluoroacetic acid
THF	Tetrahydrofuran
TLC	Thin layer chromatography
UV	Ultraviolet

List of figures

List of schemes

Chapter 1: Introduction

The interactions and functions of proteins can only be understood by studying their localization, interactions, and activities *in vivo* and *in vitro*. SNAP-tag technology was developed based on the reaction of the human DNA repair protein (hAGT) with O^6-benzylguanine (BG) derivatives and is a protein-labelling technique which allows for specific labelling of proteins with effector molecules containing a BG moeity[1–3]. Besides the labelling being very specific, it is covalent and irreversible. Provided the label contains BG, the labelling reaction does not depend on the nature of the label which opens a large scope for the development of new labels that can be covalently attached to a protein[3,4]. Previously available labelling methods have unpredictable side effects on the stability, solubility and affinity of the modified proteins[4].

Biomarkers can indicate the onset and/or progression of a disease in several therapeutic areas, and the ability to simultaneously detect multiple biomarkers in an individual cell is an area which has continuously been investigated. Broadly defined, a biomarker is a characteristic protein, gene or small molecule which can be measured and evaluated as an indicator of normal biological processes, pathogenic processes or pharmacological responses to a therapeutic intervention[5,6]. Mass cytometry has been developed as an approach in which metal-chelating polymers (MCPs) are used to label antibodies with multiple metal ions to achieve a multiplex analysis using inductively coupled plasma mass spectrometry (ICP-MS) to qualitatively and quantitatively detect specific features in/on a specific cell[7–10].

Both SNAP-tag technology and the use of MCPs as protein-tags in mass cytometry act as inspiration for our project. We aim to exploit reversible addition-fragmentation chain-transfer (RAFT) polymerization to develop a universal approach for the synthesis of polymeric tags able to conjugate to proteins via SNAP-tag technology. Chapter 2 of this thesis presents an overview of the relevant background, with emphasis on the development of mass cytometry and SNAP-tag technology. In Chapter 3, the synthesis of a novel RAFT agent and its use as a facile route to synthesize a polymer with an α-O^6-benzylguanine chain-end is presented. Chapter 4 briefly discusses MCPs and subsequently presents evidence that pendant groups of the acrylate-based polymer with an α-O^6-benzylguanine chain-end can be modified to contain

metal-chelating ligands without altering the α-chain-end. We also investigate the ability to modify the ω-chain end of RAFT generated polymers by attaching a maleimide-functional fluorescent dye. Finally, Chapter 5 discusses the implications of this work as well as some of the opportunities it unwraps for future work.

1.1. References

(1) Juillerat, A.; Heinis, C.; Sielaff, I.; Barnikow, J.; Jaccard, H.; Kunz, B.; Terskikh, A.; Johnsson, K. *ChemBioChem* **2005**, *6* (7), 1263–1269.

(2) Keppler, A.; Gendreizig, S.; Gronemeyer, T.; Pick, H.; Vogel, H.; Johnsson, K. *Nat. Biotechnol.* **2002**, *21* (1), 86–89.

(3) Johnsson, N.; Johnsson, K. *ChemBioChem* **2003**, *4* (9), 803–810.

(4) Kampmeier, F.; Ribbert, M.; Nachreiner, T.; Dembski, S.; Beaufils, F.; Brecht, A.; Barth, S. *Bioconjug. Chem.* **2009**, *20* (5), 1010–1015.

(5) Strimbu, K.; Tavel, J. a. *Curr Opin HIV AIDS* **2011**, *5* (6), 463–466.

(6) Richter, W. S. *Eur. J. Nucl. Med. Mol. Imaging* **2006**, *33* (SUPPL. 13).

(7) Lou, X.; Zhang, G.; Herrera, I.; Kinach, R.; Ornatsky, O.; Baranov, V.; Nitz, M.; Winnik, M. A. *Angew. Chemie - Int. Ed.* **2007**, *46* (32), 6111–6114.

(8) Majonis, D.; Herrera, I.; Ornatsky, O.; Schulze, M.; Lou, X.; Soleimani, M.; Nitz, M.; Winnik, M. A. *Anal. Chem.* **2010**, *82* (21), 8961–8969.

(9) Bandura, D. R.; Baranov, V. I.; Ornatsky, O. I.; Antonov, A.; Kinach, R.; Lou, X.; Pavlov, S.; Vorobiev, S.; Dick, J. E.; Tanner, S. D. *Anal. Chem.* **2009**, *81* (16), 6813–6822.

(10) Ornatsky, O.; Bandura, D.; Baranov, V.; Nitz, M.; Winnik, M. A.; Tanner, S. *J. Immunol. Methods* **2010**, *361* (1–2), 1–20.

Chapter 2: Historical and theoretical background

2.1. Introduction

There has long been a desire for simultaneous and quantitative analysis of many biomarkers in an individual cell to identify the presence and proportions of various populations of interest. A variety of methods have been developed, based on the detection of molecules of interest (antigens) using antibodies, to shed light on the complexity of cellular systems[1]. An epitope is any structure or sequence found on an antigen that is recognized by an antibody (Figure 2.1), and attaching a detectable label to the antibody enables analysis of the epitopes present[1,2]. Various labels have been used[3], the most significant of which was the discovery of fluorescent protein reporters. The attachment of a fluorescent probe in combination with fluorescent microscopy remains the imaging technique of choice for most researchers[4]. Unfortunately spectral overlap is inevitable when using multiple fluorescent dyes[5]. For high-throughput multi-parametric analysis of individual cells, flow cytometry and mass cytometry have become the methods of choice[6–9].

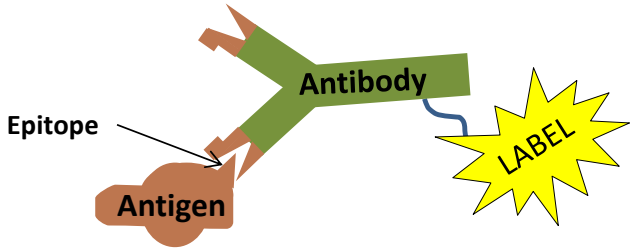

Figure 2.1: Graphical representation of a compatible epitope and antibody combination.

In this chapter we present various developments which have inspired the research we present in this thesis. We provide a brief overview of protein-labelling – with specific focus on the development of SNAP-tag technology. This is followed by a discussion of flow cytometry – a technique which led to the development of mass cytometry and the subsequent development of metal-chelating polymers (MCPs) used to label proteins[9]. Finally, we briefly discuss the possibility of exploiting electron microscopy in conjunction with MCP-based protein labels to develop a high resolution spatial cell imaging technique.

2.2. Protein labelling

Specific labelling of proteins with synthetic reporter molecules provides exciting tools in studying protein function, localization, interactions and activities. This promises to have a large impact on drug development. Fusion of a fluorescent protein to a protein of interest has already revealed a wealth of information on many biological systems[10,11], however the attachment of different molecular labels offer a broad range of properties and functionalities[11–13]. Reactive chemical groups, fluorophores, pharmacologically active compounds, or any number of compatible functionalities can be attached to a protein of interest.

An ideal protein labelling method has the following features[14]:

- The possibility to introduce a label of choice in one step.
- Fast and quantitative labelling.
- No labelling of non-target proteins.
- A small tag to minimize impact on the protein function.
- Formation of a stable, covalent bond between protein and label.
- The reagents used for labelling should have no side effects.

Many available labelling methods are accompanied by unpredictable side effects on the stability, solubility and affinity of modified proteins[15,16]. *In vivo* labelling is generally noncovalent, focussing on the formation of complexes[16]. Traditionally, most strategies have been based on genetically fusing a reporter molecule to the protein of interest which is applicable only to a limited class of proteins, and achieving site-specificity is complex [10].

Tag-mediated protein labelling is conditioned upon interactions between matching tags instead of purely random interactions. Tag-mediated labelling methods can be classified into three families: self-labelling tags, self-labelling proteins and enzyme-mediated labelling of tags. Self-labelling tags and proteins react directly with the labelling compound and if the labelling molecule is permeable to the cell membrane, proteins can be labelled inside the cell.

Self-labelling proteins generally have a higher specificity, but come at the cost of a larger tag which is more likely to influence protein function. In enzyme-mediated labelling, an enzyme is required to covalently link the label to the tag, providing both specificity and a small tag size. However, this is generally restricted to labelling cell surface proteins[14].

Detailed overviews of chemical labelling strategies are available[11–14,17]. The self-labelling tetracysteine tag was the first developed for specific protein labelling and is the most established method of small fluorescent tag labelling in cells[11,14]. SNAP-tag and HaloTag are the most widely used self-labelling proteins. Their labelling is irreversible and quantitative, and the main advantages are the high speed and specificity of the reaction. These self-labelling proteins have been shown to not only work within cells, but also in subcellular compartments[12–14].

2.2.1. SNAP-tag

SNAP-tag is a modified version of the human DNA-repair enzyme which was developed by Johnsson and co-workers[16]. The human DNA-repair enzyme, O^6-alkylguanine alkyltransferase (hAGT), recognizes O^6-alkylated guanine in DNA and irreversibly transfers the alkyl group to one of its reactive cysteine group residues, yielding repaired DNA and alkylated hAGT (Scheme 2.1)[18]. Researchers found that when O^6-benzylguanine (BG) derivatives are introduced into cells, the benzyl group is readily transferred to the hAGT. BG derivatives can thus be used to specifically label proteins fused to hAGT (Scheme 2.1)[16,19]. Mutants of hAGT with significantly increased reactivity towards BG substrates have been engineered[20,21]. These mutant proteins (SNAP-tag) react 50-fold faster than human AGT, are slightly smaller, more resistant to oxidation and do not bind to DNA[12]. They allow for a highly efficient, covalent and irreversible labelling of hAGT fusion proteins.

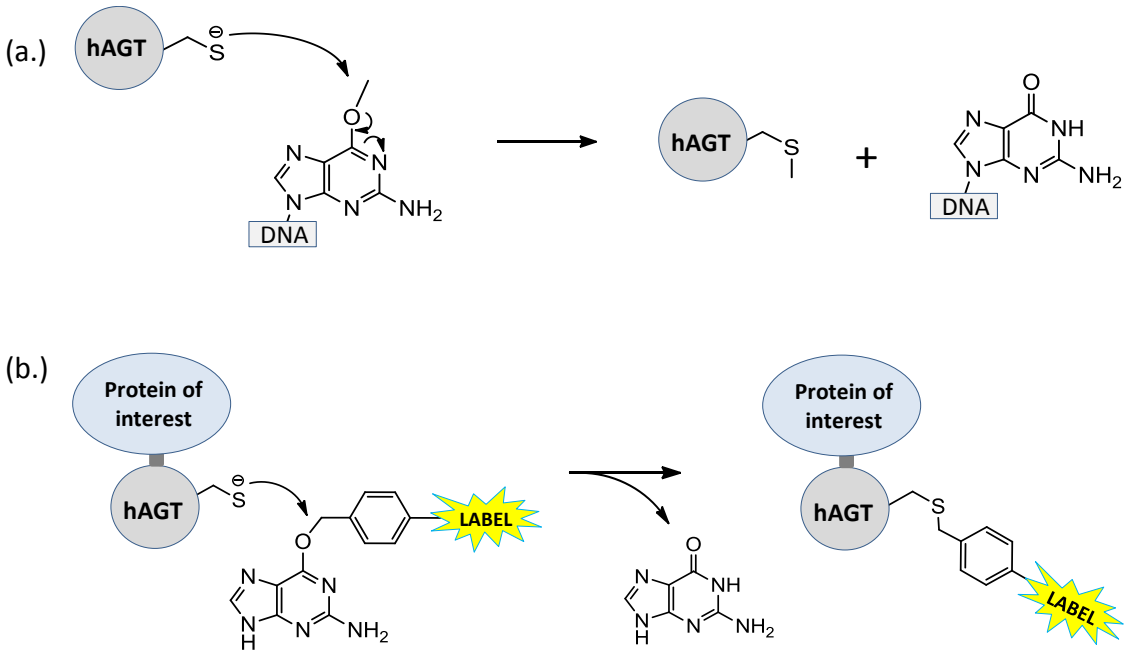

Scheme 2.1: The human repair enzyme (hAGT) reacts covalently and irreversibly with (a.) O^6-alkylated guanine in DNA and (b.) O^6-benzylguanine derivatives[20].

BG derivatives have been used for the *in vivo* and *in vitro* labelling of hAGT fusion proteins[16,19]. SNAP-tag technology has major advantages. The reaction does not depend on the nature of the label and so allows coupling with a fusion partner containing various effector molecules. The coupling is rapid, site-directed and covalent, and BG shows no significant reactivity to proteins other than hAGT[21].

2.3. Flow cytometry

Flow cytometry is a powerful technique for the analysis of multiple parameters of individual cells within heterogeneous populations. A flow cytometer performs analysis by passing thousands of fluorescently tagged cells per second through a laser beam. As samples are delivered hydrodynamic focussing ensures that cells pass through the laser beam one at a time. As a cell passes through the laser, it scatters light at all angles (Figure 2.2). The magnitude of forward scatter is roughly proportional to the size of the cell, while side scatter is a measure of the internal complexity of the cell. Fluorophore-labelled antibodies are added to the cell sample and they bind to specific antigens on the cell surface or in the cell. As laser light of the right wavelength strikes the fluorophore, a fluorescent signal is emitted which travels along the same path as the side scattered signal. The signal is directed through a series

of appropriate filters and mirrors delivering particular wavelength ranges to the appropriate detectors. A lot of information can be derived about the size, shape, and properties of the cells which have been labelled with fluorescent tags.

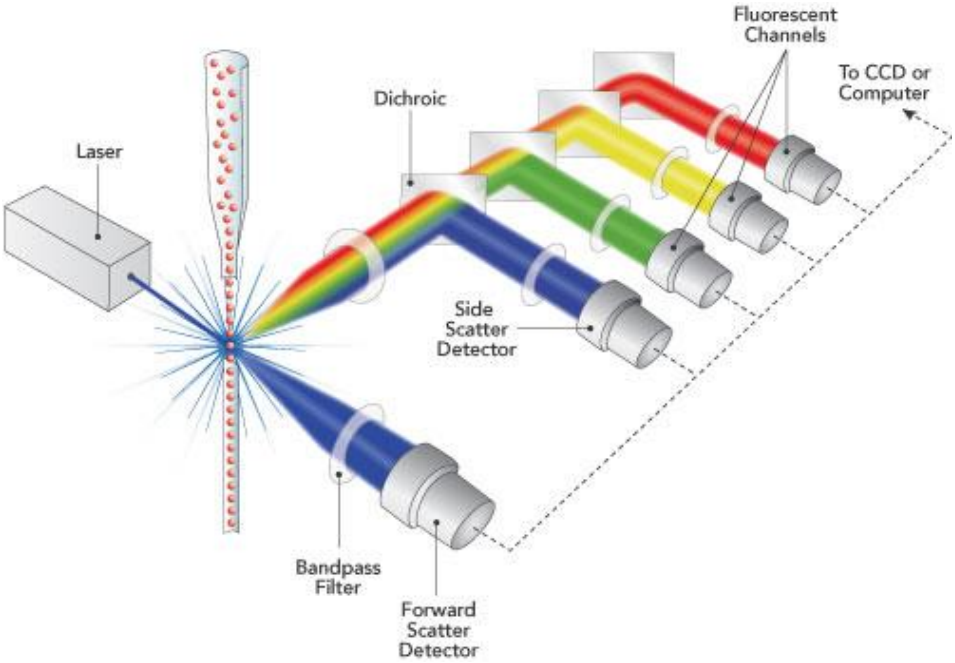

Figure 2.2: Primary systems of the flow cytometer. Fluidics system (flow cell), lasers, optics, detectors, electronics and the peripheral computer system[22].

For some time, flow cytometry stagnated at 4 colour analysis in most laboratories due to limitations related to instrumentation. Significant advances in hardware, software and reagents for flow cytometry led to the development of an 8 colour, 10-parameter system by the late 1990s[23]. Modern flow cytometry is generally limited to 10 simultaneous measurements, but the frontiers have been pushed and an instrument able to measure 19 parameters[7] at more than 10 000 cells/s has been shown. The emission bands of fluorescence are wide enough that spectral overlap is inevitable when making simultaneous measurements with multiple dyes. While advanced fluorescent imaging techniques are available[5,23–25], the main limitation when employing fluorescence remains the spectral overlap of fluorescent labels[5,23,26,27].

2.4. Mass cytometry

Immunophenotyping by mass cytometry is a new technology that couples flow cytometry with mass spectrometry, offering single-cell analysis of at least 45 simultaneous parameters without fluorescent agents at a rate of 1000 cells/s[28]. In the place of fluorescent markers, mass cytometry uses specially designed multi-atom elemental tags attached to antibodies which are detected using the high resolution, sensitivity and speed of analysis of inductively coupled plasma time-of-flight mass spectrometry (ICP-TOF-MS)[26–28]. Mass cytometry does not have the interference of spectral overlap associated with fluorescent imaging, and allows for a greater depth and breadth of phenotypic and functional cytometric profiling.

2.4.1. Detection in mass cytometry

Mass spectrometry functions by ionizing chemical compounds to generate charged molecules or molecule fragments and measuring their mass-to-charge ratio. ICP-MS is the most advanced and sensitive means of detecting the elemental composition of materials. In ICP-MS the ionization is achieved by a high-temperature ICP source and the ions separated and detected by a mass spectrometer. It has been used for ultra-trace (10^{-15} g/mL) detection of metals and other elements[28].

Bandura *et al.*[8] described the detailed instrumental design considerations for a purpose-designed prototype mass cytometer for the real-time analysis of individual biological cells. Cells are ‘stained’ with target-specific, multi-atom elemental tags attached to antibodies. Cells in a single-cell suspension pass into a nebulizer placing the cells into droplets to be introduced to the mass cytometer. The cells travel through argon plasma where the sample disintegrates and atoms/molecular fragments are ionized and then analysed by TOF-MS – plotting mass-to-charge ratio and the counts of each ion. Mass cytometry has practically no overlap between detection channels and can provide absolute quantification[8,9,26–28].

2.4.2. Development of elemental tags based on metal-chelating polymers

To overcome the limitations associated with the spectral overlap of fluorescent tags, multi-atom elemental tags consisting of metal-chelating polymers were developed[29]. Mass

spectrometry is able to discriminate stable isotopes of different atomic masses with high accuracy. In 2002, Baranov *et al.*[30] reported novel immunoassays where epitopes of interest were tagged with antibodies attached to specific elements and the elemental component quantified by ICP-MS. Multiple tagging with a single isotope linearly improves the detection limit, and thus the use of a metal-chelating polymeric tag (Figure 2.3) increased the sensitivity of detection by incorporating multiple numbers of a given ion on one tag[29].

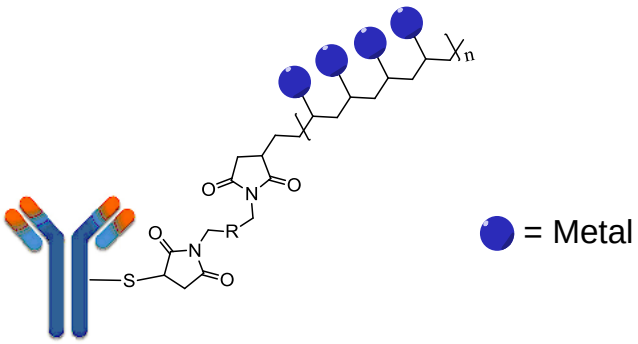

Figure 2.3: Metal-chelating polymer attached to an antibody via the maleimide chain-end.

Elemental tags based on a water soluble polymer with multiple metal-chelating ligands were designed[9,29]. The chelating ligands (1,4,7,10-tetraazocyclodecan-1,4,7,10-tetraacetic acid (DOTA) and diethylenetriaminepentaacetic acid (DTPA)) were chosen to form high-affinity complexes with lanthanide (Ln^{3+}) ions. Selection of the lanthanides and their various isotopes proved to be extremely useful as they have similar coordination chemistry, low natural abundance and have masses in a useful range for MS-detection (*m/z* from 100 to 200) allowing the synthesis of a large number of different tags.

A functional metal-chelating polymer was designed[9] to increase the number and density of metal ions per polymer. The new polymer was designed around several requirements which would further increase sensitivity and ultimately lead to the development of quantitative mass cytometry[9]. The polymer required the following:

- A metal chelating ligand on every repeat unit.
- Degree of polymerization above 60.
- Narrow molar mass distribution.
- Chain-end functionality suitable for antibody attachment.

Reversible addition-fragmentation chain transfer (RAFT) polymerization assists the development of polymers that meet these design requirements[31–33]. Careful selection of the RAFT agent enables the synthesis of polymers with a low dispersity and end-group functionality. End-functional polymers are synthesized by inserting functionality on the RAFT agent R-group, or by post-polymerization modification of the ω-chain-end[31,32,34,35].

In the development of a polymer that satisfies these requirements, the cheap and easily modifiable monomer, *tert*-butyl acrylate, was polymerized using di-1-phenylethyl trithiocarbonate as RAFT agent[9]. The butyl acrylate groups were deprotected to form poly(acrylic acid) followed by a coupling reaction with *t*-BOC-ethylenediamine and the subsequent deprotection of the BOC groups to yield an amino polymer. This was followed by the attachment of a DTPA ligand to each repeat unit. The poly(DTPA) chains were modified to have a maleimide end-group (Scheme 2.2). Antibody conjugation is attained by treating the antibody with tris(2-carboxyethyl)phosphine (TCEP) to partially reduce hinge region disulfides to thiols. The thiol groups can undergo Michael addition with α,β-unsaturated carbonyl compounds, such as (in this case) the maleimide.

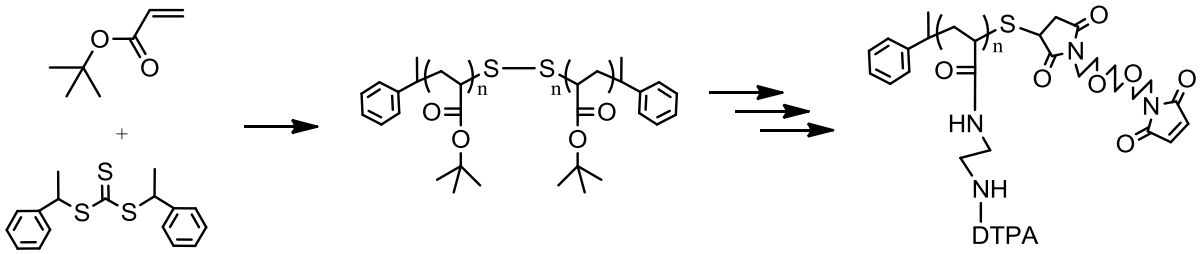

Scheme 2.2: Scheme depicting the general synthetic route of poly(*t*-butyl acrylate), followed by modifications towards a metal-chelating polymer with maleimide end-group.

The number of DTPA ligands was determined by ^{1}H NMR, and the number of lanthanide ions per polymer was determined by isothermal titration calorimetry (ITC)[36,37]. The number of metal atoms carried by each antibody was determined with a combination of UV/vis spectroscopy and ICPMS and combining these results with the number of metals per polymer, they were able to determine that 2.4 ± 0.3 polymer chains were attached to each antibody[9]. Eleven different monoclonal antibodies were each labelled with a different lanthanide-chelated tag. The labelled, monoclonal, metal-tagged antibodies were used to

obtain an 11-plex mass cytometric assay to determine the main types of cells present in a small amount of whole umbilical cord blood[9].

In mass cytometry the entire cell is disintegrated to obtain information and while the technique overcomes the limitation imposed by the spectral overlap on fluorescent imaging, we would be very interested to investigate a spatial cell-imaging technique using tags based on metal-chelating polymers and the resolution offered by scanning electron microscopy (SEM).

2.5. SEM-EDS

Energy-dispersive X-ray spectroscopy (EDS, EDX, or EDXS) is an analytical technique used for elemental analysis or chemical characterization of a sample. Every element has characteristic X-ray lines which result from electron transitions between inner orbitals. An electron needs to be removed to create a vacancy into which another electron can fall, and these vacancies can be produced by electron bombardment. An energy-dispersive (ED) spectrum gives the X-ray energy (eV) on the x-axis and number of counts on the y-axis. EDS used in conjunction with advanced SEM can provide high-resolution imaging, semi-quantitative elemental analysis, and qualitative X-ray elemental maps[38].

2.6. Our proposal/intended goals

The metal-chelating polymer synthesis published by Majonis and co workers[9] for the use in quantitative mass cytometry has many benefits, which we hope to exploit. We aim to synthesize a similar metal-chelating polymer, but with the ability to be conjugated to an antibody *via* SNAP-tag. To achieve this, we aimed to synthesize a novel RAFT chain transfer agent with O^6-benzylguanine functionality which would facilitate the facile synthesis of a polymer with an α-BG chain-end. The α-BG chain-end allows specific, irreversible and quantitative binding of a tag to an antibody via SNAP-tag and the ω-chain-end of the RAFT-generated polymer can be modified post-polymerization.

Fluorescence microscopy has been used for spatial imaging of cells, however this remains limited by spectral overlap. Mass cytometry has overcome the limitation of spectral overlap, but tagged cells are disintegrated during imaging/detection. We aim to overcome these limitations by tagging a cell surface with antibody-MCP conjugates in order to investigate high-resolution, spatial cell-imaging by overlaying SEM and EDS data. Attaching a fluorescent dye to the ω-chain-end of the MCP will allow us to directly compare the resolution of fluorescence microscopy and SEM-EDS.

2.7. References

(1) Brizzard, B. *BioTechniques*. **2008**, *44* (5), 693–695.

(2) Jarvik, J. W.; Telmer, C. A. *Annu. Rev. Genet.* **1998**, *32*, 601–618.

(3) Tsien, R. Y. *Annu. Rev. Biochem.* **1998**, *67* (1), 509–544.

(4) Duwé, S.; Dedecker, P. *Nat. Methods* **2017**, *14* (11), 1042–1044.

(5) Roederer, M. *Cytometry* **2001**, *45* (3), 194–205.

(6) Stewart, C. C. *J. Immunoassay* **2000**, *21* (2), 255–272.

(7) Perfetto, S. P.; Chattopadhyay, P. K.; Roederer, M. *Nat. Rev. Immunol.* **2004**, *4* (8), 648–655.

(8) Bandura, D. R.; Baranov, V. I.; Ornatsky, O. I.; Antonov, A.; Kinach, R.; Lou, X.; Pavlov, S.; Vorobiev, S.; Dick, J. E.; Tanner, S. D. *Anal. Chem.* **2009**, *81* (16), 6813–6822.

(9) Majonis, D.; Herrera, I.; Ornatsky, O.; Schulze, M.; Lou, X.; Soleimani, M.; Nitz, M.; Winnik, M. A. *Anal. Chem.* **2010**, *82* (21), 8961–8969.

(10) Johnsson, N.; Johnsson, K. *ChemBioChem* **2003**, *4* (9), 803–810.

(11) Lin, M. Z.; Wang, L. *Physiology* **2008**, *23* (3), 131–141.

(12) O'Hare, H. M.; Johnsson, K.; Gautier, A. *Current Opinion in Structural Biology*. **2007**, *17* (4), 488–494.

(13) Sletten, E. M.; Bertozzi, C. R. *Angew. Chemie - Int. Ed.* **2009**, *48* (38), 6974–6998.

(14) Hinner, M. J.; Johnsson, K. *Curr. Opin. Biotechnol.* **2010**, *21* (6), 766–776.

(15) Kampmeier, F.; Ribbert, M.; Nachreiner, T.; Dembski, S.; Beaufils, F.; Brecht, A.; Barth, S. *Bioconjug. Chem.* **2009**, *20* (5), 1010–1015.

(16) Keppler, A.; Gendreizig, S.; Gronemeyer, T.; Pick, H.; Vogel, H.; Johnsson, K. *Nat. Biotechnol.* **2002**, *21* (1), 86–89.

(17) Liu, C. C.; Schultz, P. G. *Annu. Rev. Biochem.* **2010**, *79* (1), 413–444.

(18) Pegg, A. E. *Mutation Research - Reviews in Mutation Research*. **2000**, *462* (2), 83–100.

(19) Keppler, A.; Kindermann, M.; Gendreizig, S.; Pick, H.; Vogel, H.; Johnsson, K.

Methods **2004**, *32* (4), 437–444.

(20) Piast, M.; Kustrzeba-Wójcicka, I.; Matusiewicz, M.; Banaś, T. *Acta Biochim. Pol.* **2005**, *52* (2), 507–513.

(21) Kindermann, M.; George, N.; Johnsson, N.; Johnsson, K. *J. Am. Chem. Soc.* **2003**, *125* (26), 7810–7811.

(22) Semrock. Flow Cytometry Core Facility https://www.semrock.com/flow-cytometry.aspx (accessed Dec 1, 2017).

(23) Roederer, M.; De Rosa, S.; Gerstein, R.; Anderson, M.; Bigos, M.; Stovel, R.; Nozaki, T.; Parks, D.; Herzenberg, L.; Herzenberg, L. *Cytometry* **1997**, *29* (4), 328–339.

(24) Gratama, J. W.; D'Hautcourt, J. L.; Mandy, F.; Rothe, G.; Barnett, D.; Janossy, G.; Papa, S.; Schmitz, G.; Lenkei, R. *Cytometry* **1998**, *33* (2), 166–178.

(25) Bastiaens, P. *Trends Cell Biol.* **1999**, *9* (2), 48–52.

(26) Ornatsky, O.; Bandura, D.; Baranov, V.; Nitz, M.; Winnik, M. A.; Tanner, S. *J. Immunol. Methods* **2010**, *361* (1–2), 1–20.

(27) Spitzer, M. H.; Nolan, G. P. *Cell* **2016**, *165* (4), 780–791.

(28) Bendall, S. C.; Nolan, G. P.; Roederer, M.; Chattopadhyay, P. K. *Trends Immunol.* **2012**, *33* (7), 323–332.

(29) Lou, X.; Zhang, G.; Herrera, I.; Kinach, R.; Ornatsky, O.; Baranov, V.; Nitz, M.; Winnik, M. A. *Angew. Chemie - Int. Ed.* **2007**, *46* (32), 6111–6114.

(30) Baranov, V. I.; Quinn, Z.; Bandura, D. R.; Tanner, S. D. *Anal. Chem.* **2002**, *74* (7), 1629–1636.

(31) Moad, G.; Rizzardo, E.; Thang, S. H. *Aust. J. Chem.* **2005**, *58* (6), 379–410.

(32) Perrier, S.; Takolpuckdee, P.; Westwood, J.; Lewis, D. M. *Macromolecules* **2004**, *37* (8), 2709–2717.

(33) Mayadunne, R. T. A.; Rizzardo, E.; Chiefari, J.; Krstina, J.; Moad, G.; Postma, A.; Thang, S. H. *Macromolecules* **2000**, *33* (2), 243–245.

(34) Willcock, H.; O'Reilly, R. K. *Polym. Chem.* **2010**, *1* (2), 149–157.

(35) Keddie, D. J.; Moad, G.; Rizzardo, E.; Thang, S. H. *Macromolecules* **2012**, *45* (13), 5321–5342.

(36) Darras, V.; Nelea, M.; Winnik, F. M.; Buschmann, M. D. *Carbohydr. Polym.* **2010**, *80* (4), 1137–1146.

(37) Gouin, S.; Winnik, F. M. *Bioconjug. Chem.* **2001**, *12* (3), 372–377.

(38) Goldstein, G.; Newbury, D.; Echlin, P.; Joy, D.; FIori, C.; Lifshin, E. *Scanning electron microscopy and microanalysis*; Plenum Press: New York, 1981.

Chapter 3: Synthesis of a trithiocarbonate RAFT agent with *O*^{6}-benzylguanine functionality.

3.1. Introduction

In recent years, reversible addition-fragmentation chain transfer (RAFT) polymerization has become one of the most powerful and utilized methods in the field of reversible deactivation radical polymerization (RDRP)[1,2]. The careful design of chain transfer agents (CTAs) has led to numerous possibilities in the design of speciality polymers. From the synthesis of compounds with specific functionalities built into polymer backbones or chain ends, to the synthesis of molecules with complex architectures, RAFT polymerization has played a leading role in the evolution of polymer chemistry[1–6].

Careful choice of RAFT agent allows control over the molecular weight and end-group functionality of polymers. The four classes of CTAs (dithioesters, trithiocarbonates, dithiocarbamates and xanthates) differ by the substituent group next to the C=S functionality – labelled Z and R[1,3]. The Z-group activates the C=S bond and stabilizes the intermediate radical, affecting reactivity to the incoming radical. The R-group is chosen as a good leaving group and should be capable of reinitiating chains. The R-group is found at the α-chain-end and the Z-group at the ω-chain-end of the polymer. End-functionalized polymers can be achieved either by inserting functionality into the RAFT agent (generally the R-group), or by post-polymerization modifications (generally the Z-group)[1,7–9].

RAFT polymerization has provided an adaptable platform for the controlled synthesis of polymers for biological applications[7]. Careful design of the RAFT agent allows the installation of bio-relevant functionality into the R-group, for example a biotinylated trithiocarbonate RAFT agent was synthesized by Hong and Pan[10]. In this chapter we report the design of a trithiocarbonate RAFT agent with *O*^{6}-benzylguanine functionality on the R-group. SNAP-tag fusion proteins attach rapidly, specifically, covalently and irreversibly to substrates with O6-benzylguanine (BG) functionality[11,12] (Scheme 3.1) and these have been shown to be efficient for labelling with small molecules both *in vivo* and *in vitro*[12–16].

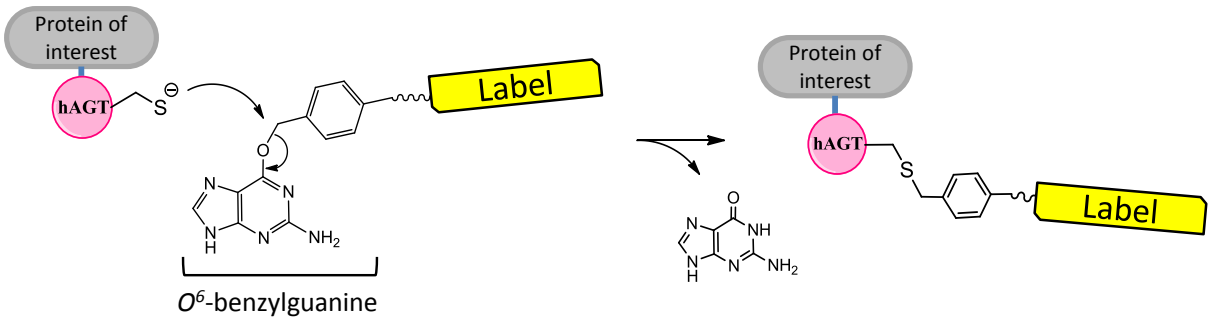

Scheme 3.1: Attaching a label to a fusion protein through SNAP-Tag.

A RAFT agent with BG functionality allows the facile synthesis of polymers with α-chain-end BG functionality, which can subsequently be employed as protein labels used in conjunction with SNAP-tag. The synthesis of our RAFT agent comprises the synthesis of an *O*^{6}-benzylguanine moiety and its incorporation into a trithiocarbonate RAFT agent via a triazole linker. In general, trithiocarbonate RAFT agents are known to be compatible with the polymerization of styrenic and acrylic monomers. We introduce here a universal technique for the synthesis of polymeric SNAP-tag labels by RAFT polymerization.

3.2. Results and discussion

3.2.1. Synthesis of O^6-(*p*-azidobenzyl)guanine derivative

A trithiocarbonate RAFT agent with a (1-phenyl-1H-1,2,3-triazole-4-yl)methyl leaving group was introduced by Akeroyd *et al*[18]. The triazole moiety was introduced as a linker via the Cu^I-catalyzed azide alkyne cycloaddition (CuAAC) reaction[17]. The leaving group showed good control over molar mass and dispersity in the RAFT polymerization of vinyl acetate, styrene, *n*-butyl acrylate and NVP, and it was also shown that the phenyl group was essential in achieving this control[18]. The triazole linker provides a facile route to the introduction of α-chain-end functionality through the RAFT agent R-group using an appropriate azide. In light of this we synthesized an O^6-(*p*-azidobenzyl)guanine derivative (**5** in Scheme 3.2) based on the optimized protocols for the synthesis of O^6-benzylguanine derivatives published by Keppler[12].

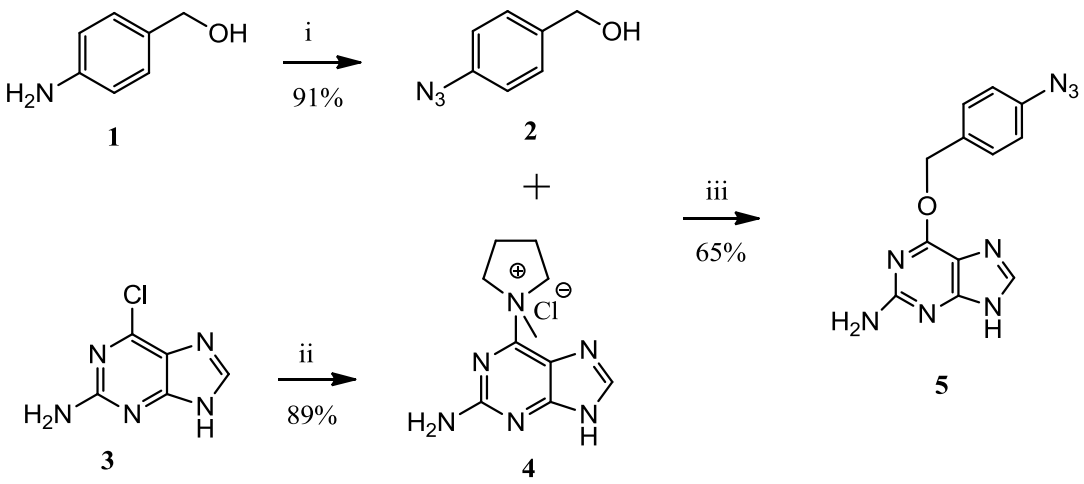

Scheme 3.2: Route to the synthesis of 6-((4-azidobenzyl)oxy-7H-purin-2-amine (**5**). (i) 1. AcOH, H_2SO_4, $NaNO_2$, H_2O, 0 °C, 5 min. 2. NaN_3, H_2O, 0 °C, 30 min. (ii) 1-methylpyrrolidine, DMF, 48 h, r.t. (iii) DMAP, DMF, 4 h, r.t.

We initially tried to synthesize **2** by nucleophilic substitution of (4-bromophenyl)methanol. ^{1}H NMR showed ~ 50 % of the halide had been converted, however we were unable to separate the product from the starting material. In a different route 4-aminobenzyl alcohol, **1**, was successfully converted to (4-azidophenyl)methanol, **2**, via the diazonium salt. Alkoxypurines have been synthesized by reacting 6-chloropurin-2-amine, **3,** with a large excess of sodium alkoxide[19–21]. We attempted a similar reaction after deprotonation of **2**, but we were unable to displace the chlorine at the 6- position. Further activation of the 6-position

has been shown to assist displacement[20,22]. We subsequently activated the 6-position of **3** using 1-methylpyrrolidine[23] to obtain **4**. The nucleophilic attack of **2** on **4** was successfully facilitated using NaH for deprotonation and DMAP as a nucleophilic catalyst to yield 6-((4-azidobenzyl)oxy-7H-purin-2-amine, **5**.

3.2.2. A model 'click' system and a test for the potential aminolysis of a trithiocarbonate RAFT agent

Meldal[24] and Sharpless[25] independently reported the efficiency of copper(I) species as catalyst in the cycloaddition of azides and terminal alkynes to specifically yield 1,4-disubstituted 1,2,3-triazoles. Cu(I)-catalyzed azide alkyne cycloaddition (CuAAC) can be conducted at low temperatures, with a low tendency for side reactions, and with good yields, while the uncatalyzed thermal cycloaddition affords both the 1,4- and 1,5-regioisomers[26]. The CuAAC reaction is classified as a "click" reaction[27].

Copper(I) can be introduced in several ways. The most common source of copper for the CuAAC reactions are copper(II) salts where copper(I) is generated in-situ by a reducing agent. The use of copper(II) sulphate pentahydrate with excess sodium ascorbate has been widely reported, and efficiently overcomes the instability attributed to the copper(I) species. The CuAAC reaction also proceeds in the presence of copper metal where the copper(I) catalyst is formed in-situ by the oxidation of the metal[26,28]. The catalytically active copper(I) species can also be added directly, however this species is very sensitive to oxidation and reaction conditions need to be well controlled. The addition of a base/ligand protects the copper(I) species from oxidation, whilst also enhancing the rate of the reaction[26,28,29]. Nitrogen-containing ligands have been popular for CuAAC. Among the most commonly used are diisopropylethylamine (DIPEA) and *N,N,N',N'',N''*-pentamethyldiethylenetriamine (PMDETA).

Before attempting to synthesize a BG-containing RAFT agent using our *O^6*-(*p*-azidobenzyl)guanine derivative (**5**), we investigated a model system (Scheme 3.3) of phenylazide (**6**) and but-3-yn-2-yl butyl carbonotrithioate (**7**) to test and optimise various conditions of the CuAAC reaction. The CuAAC reaction of **6** and **7** has previously been

performed in our group to yield a viable RAFT agent, and similar procedures were followed[18].

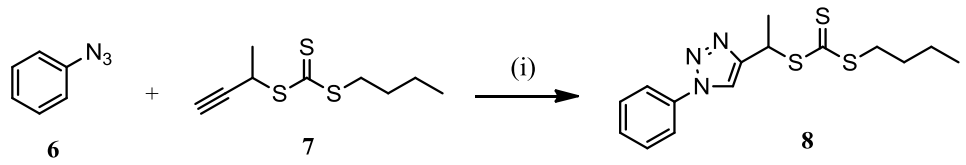

6 **7** **8**

Scheme 3.3: Synthesis of a model RAFT agent via the CuAAC reaction. (i) Various conditions were tested: (1) $CuSO_4.5H_2O$, ascorbic acid, DMF, 24h, 30° C; (2) CuBr, PMDETA, DMF, 24h, 30° C; (3) $CuBr(PPh_3)_3$, 24h, 30° C; (4) $CuBr(PPh_3)_3$, DMF, 24h, 30° C.

We investigated four systems commonly used for the CuAAC reaction. We first used $CuSO_4{\cdot}5H_2O$ as the copper source with ascorbic acid as reducing agent[18,25]. The crude ^{1}H NMR spectrum of a typical reaction showed a 60 % conversion of the starting materials. The crude product was easily purified by column chromatography (Figure 3.1). The crude ^{1}H NMR spectrum employing a system with CuBr as the copper source and PMDETA as the ligand[28] showed a near quantitative conversion and no further purification was necessary after running the reaction mixture through an aluminium oxide plug. We attempted the click reaction with $CuBr(PPh_3)_3$ as a catalyst[30] neat and also in DMF. The neat reaction showed a >99 % conversion of the alkyne to triazole, however we decided not to carry these conditions over to our BG system. Firstly, there were unwanted impurities in the aromatic region attributable to the PPh_3. Secondly, while both **6** and **7** are liquids at room temperature the *O*^{6}-(*p*-azidobenzyl)guanine derivative (**5**) is a solid with limited solubility. The reaction in DMF gave the same issue in terms of impurities.

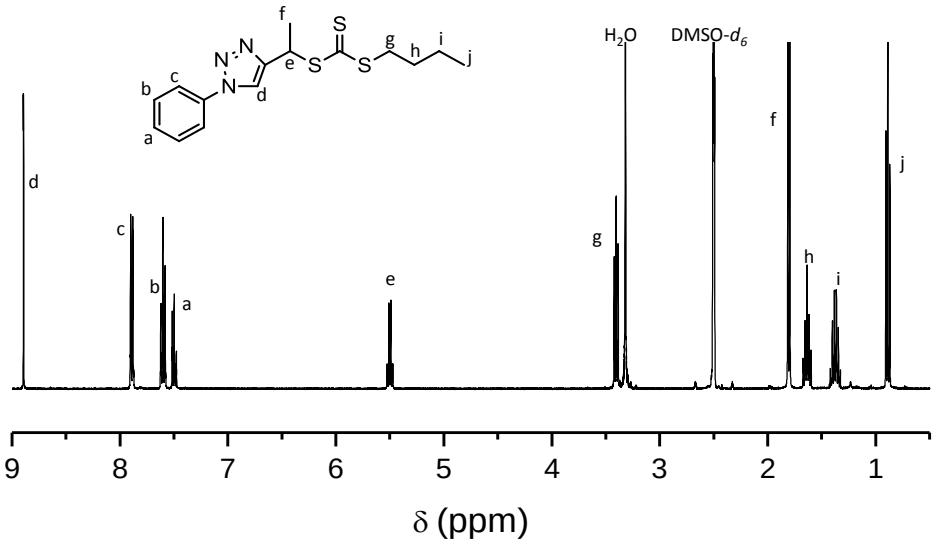

Figure 3.1: ^{1}H NMR (DMSO-d_6) spectrum of model RAFT agent (**8**).

3.2.2.1. Polymerization with model RAFT agent

Having successfully synthesized a model RAFT agent (**8**), we tested the control of the (1-phenyl-1H-1,2,3-triazol-4-yl)methyl leaving group in the polymerization of *tert*-butyl acrylate. We targeted a molecular weight of 22000 g·mol^{-1} and ^{1}H NMR of an aliquot taken before precipitation showed a conversion above 95 %. ^{1}H NMR of the synthesized poly(*tert*-butyl acrylate) (P*t*BA) confirmed the presence of the endgroup-functionality attributable to the RAFT agent. The number average molecular weight was calculated to be 23600 g.mol^{-1} with ^{1}H NMR end-group analysis (integrating 2 phenyl protons at 7.51 ppm against the single backbone proton signal at 2.1-2.4 ppm) and size exclusion chromatography (SEC) showed a dispersity of 1.19.

3.2.2.2. Test for potential aminolysis of trithiocarbonate

At present, primary and secondary amine functionalities are generally not directly accessible on RAFT agents as it leads to degradation of the RAFT agent during polymerization[7]. It was imperative to determine whether the amines present on the *O^6*-(*p*-azidobenzyl)guanine derivative (**5**) would lead to degradation (aminolysis) of a trithiocarbonate RAFT agent during polymerization. To investigate this, the model RAFT agent (**8**) and **5** were stirred together for 24 hours at room temperature and then another 24 hours at polymerization

conditions (65 °C). ^{1}H NMR showed that the trithiocarbonate remained stable in the presence of **5**.

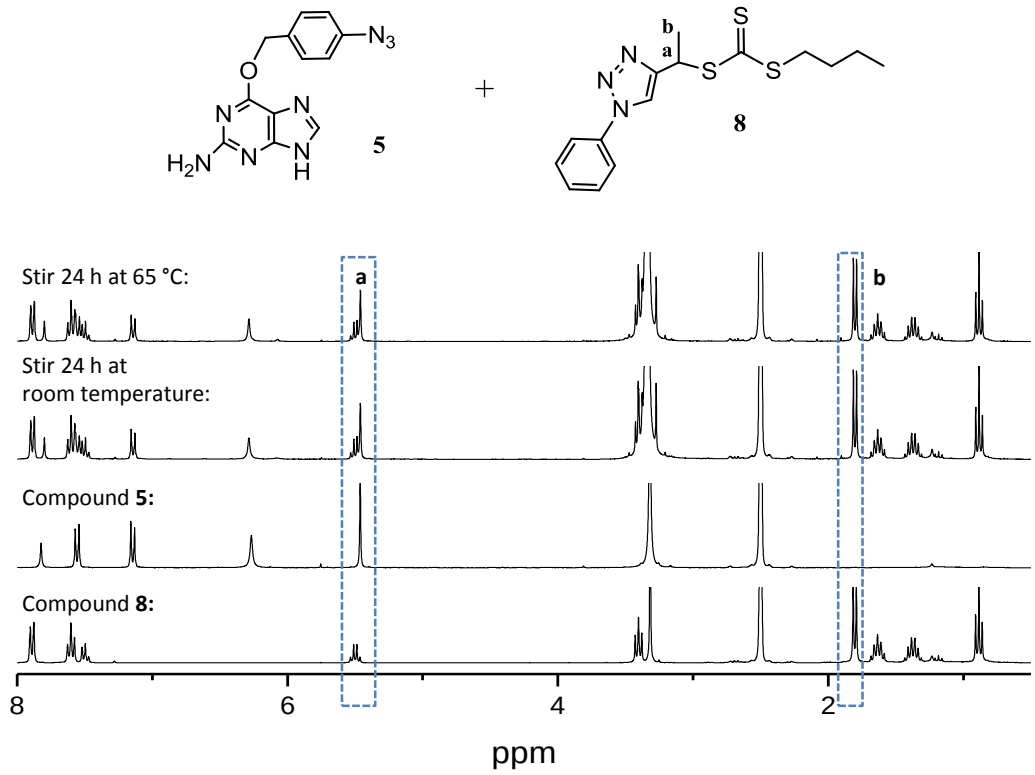

Figure 3.2: ^{1}H NMR (DMSO-d_6) spectra indicating the stability of trithiocarbonate **8** in the presence of **5**.

3.2.3. Synthesis of an α-benzylguanine trithiocarbonate RAFT agent

Having established that the amine functionalities of the guanine moiety do not harm the trithiocarbonate Z-group of the RAFT agent, the final step in the synthesis of the BG-functionalized RAFT agent was the Cu^I-catalyzed azide alkyne cycloaddition (CuAAC) of **5** and **7** to form RAFT agent **9** (Scheme 3.4).

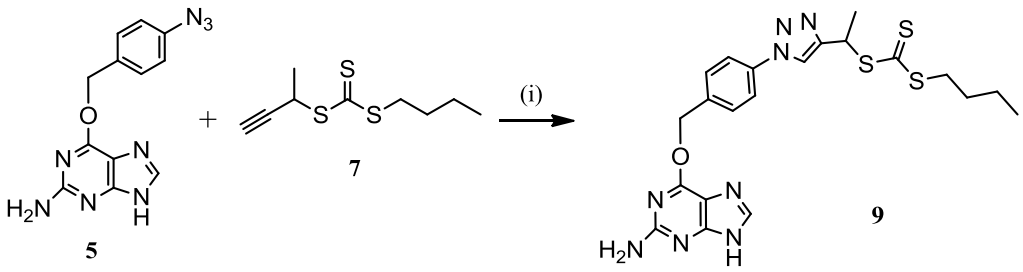

Scheme 3.4: Cu^I-catalyzed azide alkyne cycloaddition. (i) CuBr, ascorbic acid, Me_6TREN, DMF, 5 h, r.t.

We attempted the CuAAC reaction (Scheme 3.4) using the systems which had worked for the synthesis of the model RAFT agent. None of the systems showed the formation of the desired product (**9**). We subsequently focussed on the PMDETA system, increasing the amount of CuBr (up to 0.5 molar equivalent to the reactants) and reaction time (up to 72 hours) without any success. For the model click system using PMDETA and CuBr, our only purification step was the removal of the catalyst with an aluminium oxide plug. In the reaction to form **9**, ^{1}H NMR spectra before and after running the reaction mixture through an aluminium oxide plug showed a disappearance of the peaks in the aromatic region. The post-reaction removal of copper also removed the BG derivative (**5**) from the reaction mixture and we concluded that the copper(I) was complexing with **5** preferentially to the intended ligand. The copper(I) species was thus not able to catalyse the formation of the triazole linker.

We subsequently repeated the reaction using tris[2-(dimethylamino)ethyl]amine (Me_6TREN) as ligand. In comparison to the tridentate complex formed between copper(I) and PMDETA, Me_6TREN forms a stronger, more crowded, tetradentate complex with copper(I) (Figure 3.3). Consequently, the copper(I) center is more shielded from oxygen while remaining active[28,31]. We preformed the [Cu^I(Me_6TREN)]Br complex in situ in the presence of sodium ascorbate as reducing agent, before adding the alkyne, **7,** and the azide, **5**. We confirmed the formation of 1-(1-(4-(((2-amino-7H-purin-6-yl)oxy)methyl)phenyl)-1H-1,2,3-triazol-4-yl)ethyl butyl carbonotrithioate, **9**, by ^{1}H NMR, MS and the disappearance of the azide peak in the FTIR spectrum and moved on to optimizing the conversion of the azide to triazole.

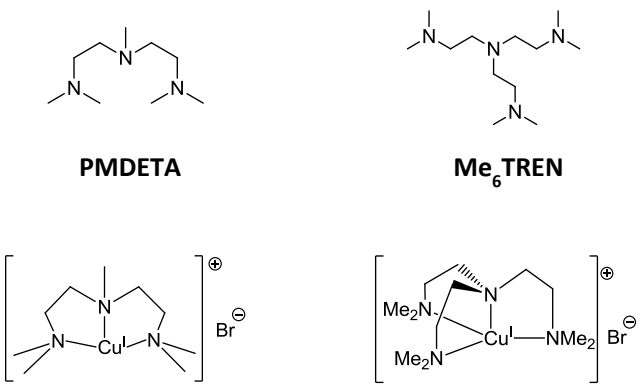

Figure 3.3: Comparison of the copper(I) complexes of PMDETA and Me_6TREN.

Following the ^{1}H NMR proton shifts of the aromatic protons from the azide (**5**), it was found that initially only around half of the azide had been converted to the triazole. This was vastly improved by increasing the ratio of the alkyne, CuBr, and Me_6TREN to that of the azide (Figure 3.4). We did not manage to achieve complete conversion. Compounds **5** and **9** proved difficult to separate and we were unable to remove all the azide (**5**). However, this problem could be overcome by adjusting polymerization calculations to account for the presence of the azide (% determined with ^{1}H NMR) as the azide would not affect the polymerization and could be removed by dialysis at a later stage.

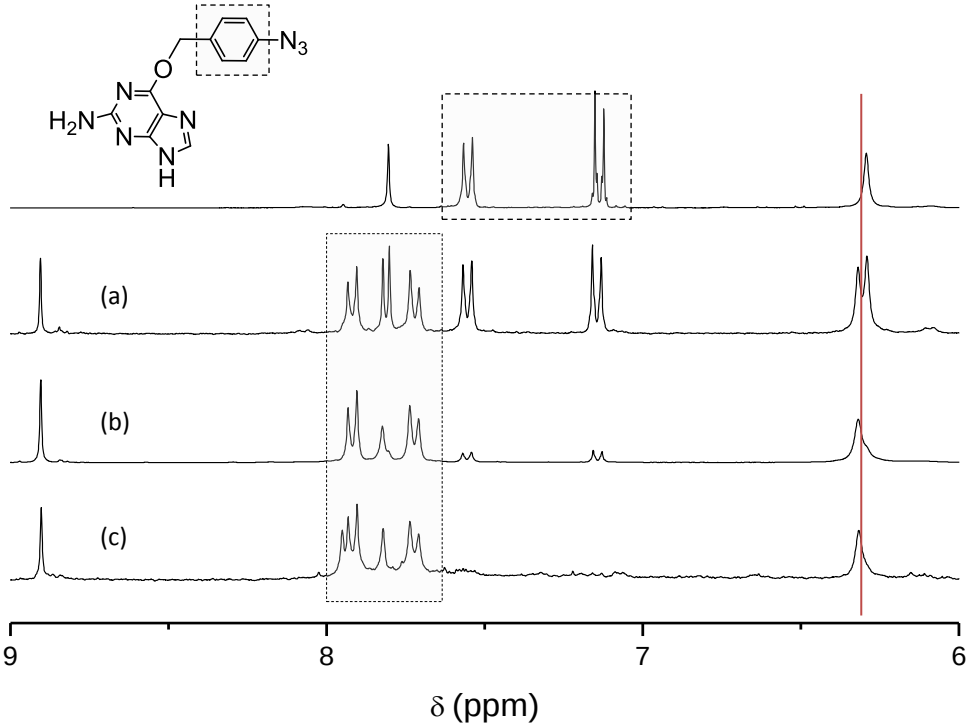

Figure 3.4: The top ^{1}H NMR (DMSO-d_6) spectrum is of O^6-(*p*-azidobenzyl)guanine (**5**) and the ensuing spectra indicate an increase in conversion of the CuAAC reaction, which can be seen by the decrease in peaks corresponding to **5,** with various ratios of azide (**5**) : alkyne (**7**) : CuBr : Me_6TREN : ascorbic acid. The following ratios were used: (a) 1 : 1 : 0.1 : 0.2 : 0.05, (b) 1 : 3 : 0.1 : 0.2 : 0.05, (b) 1 : 3 : 0.3 : 0.4 : 0.15.

Specifically considering the appearance of the triazole proton and the downfield shift of the aromatic protons, we were able to confirm the conversion of **5** to **9** by ^{1}H NMR (Figure 3.5). The homonuclear correlation spectroscopy (COSY) sequence spectrum of **9** confirmed the previous assignment of ^{1}H NMR protons (see x-axis of Figure 3.6). The gradient heteronuclear single quantum coherence (gHSQC) NMR spectrum couples carbon atoms with protons ($^1J_{C\text{-}H}$) for one bond correlation, with the ^{1}H NMR spectrum on the x-axis and the ^{13}C

NMR spectrum on the y-axis. The gHSQC spectrum (Figure 3.6) along with the gradient heteronuclear multiple bond correlation (gHMBC) spectrum (Figure 3.7) were used to confirm ^{13}C NMR assignments of **9** (see y-axis of Figure 3.7).

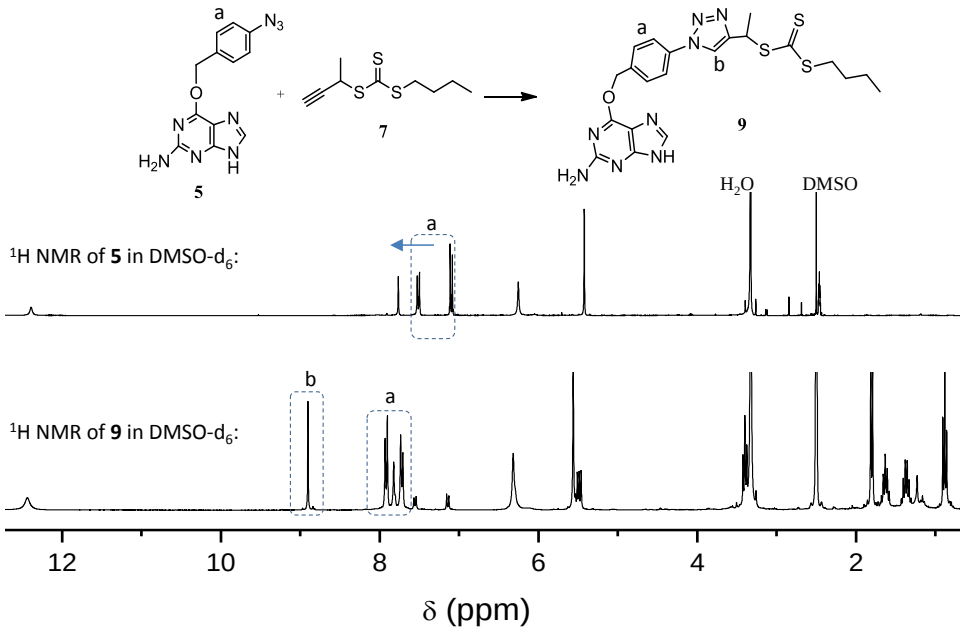

Figure 3.5: ^{1}H NMR spectra of **5** and **9** in DMSO-d$_6$.

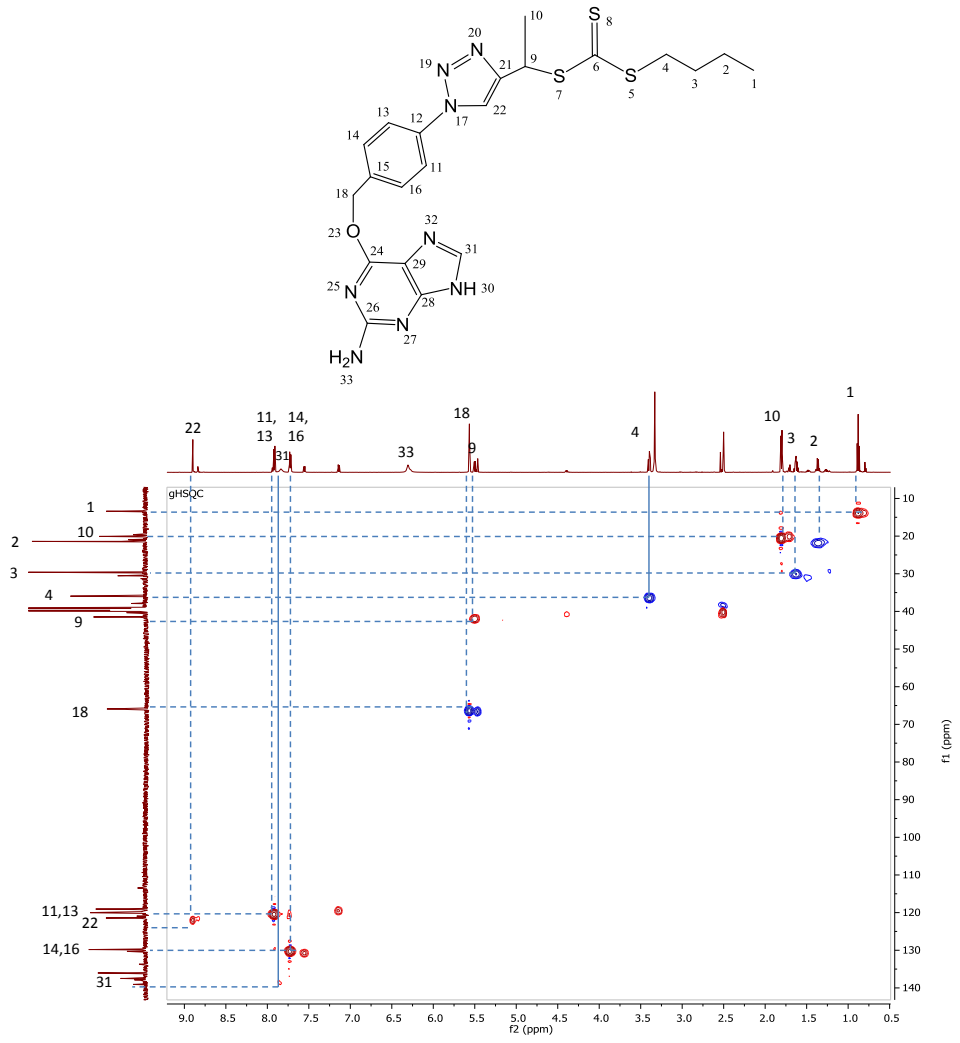

Figure 3.6: gHSQC NMR spectrum of **9** in DMSO-d_6.

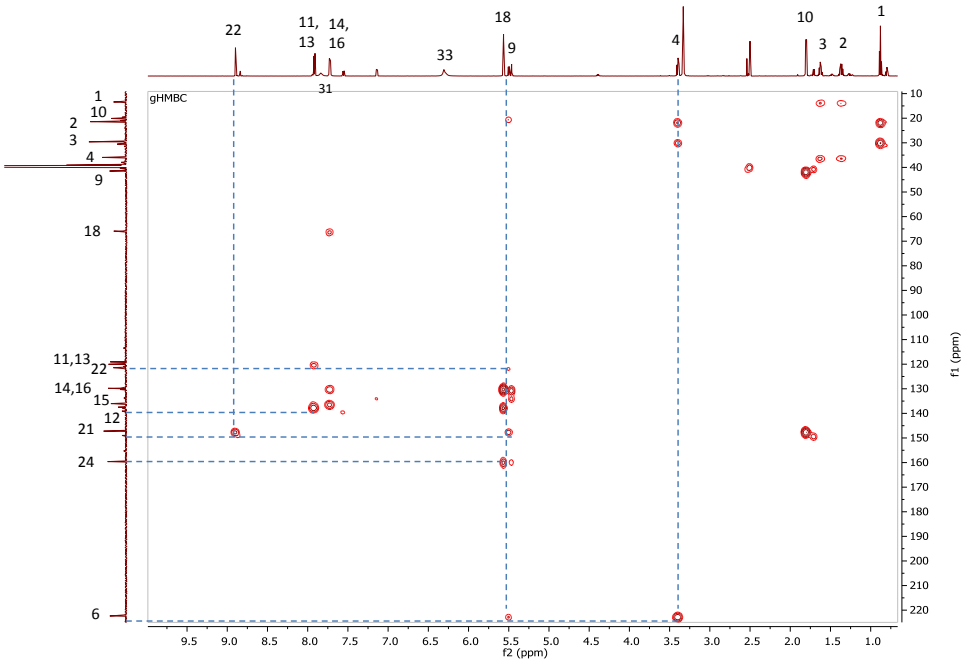

Figure 3.7: gHMBC spectrum of **9** in DMSO-d_6.

3.2.3.1. Polymerization of PtBA with the α-benzylguanine trithiocarbonate RAFT agent

To test whether **9** could successfully be used as a RAFT agent, we polymerized *tert*-butyl acrylate to yield PtBA. After precipitation and drying, ^{1}H NMR showed the expected polymer peaks as well as the presence of the RAFT agent end-groups. The achieved molecular weight was higher than expected and we attributed this to the azido-impurities in the RAFT agent. The number average molecular weight (M_n) was determined to be 34000 g·mol^{-1} with ^{1}H NMR end-group analysis by integrating the peak of the two methylene protons adjacent to the oxygen atom (a in Figure 3.8) against the signal at 2.1-2.5 ppm corresponding to 1H per polymer repeat unit (Figure 3.8). SEC (THF) showed good control with a dispersity of 1.13.

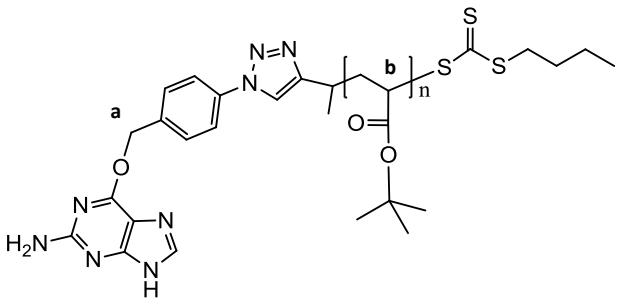

Figure 3.8: Structure of poly(*tert*-butyl acrylate) with an α-BG chain-end.

Conclusion

A novel RAFT agent with O^6-benzylguanine functionality on the R-group was developed. The initial synthesis of O^6-(*p*-azidobenzyl)guanine (**5**) proved challenging, but was achieved by activating the 6-position of 6-chloropurin-2-amine with 1-methylpyrrolidine which enabled nucleophilic substitution, in the presence of DMAP as a nucleophilic catalyst, after the deprotonation of (4-azidophenyl)methanol (**2**). It was shown that the amine functionality of benzylguanine does not lead to degradation (aminolysis) of a trithiocarbonate RAFT agent under polymerization conditions. Various catalyst systems for CuAAC reaction were successfully tested on a model system of phenylazide (**6**) and but-3-yn-2-yl butyl carbonotrithioate (**7**). These systems all failed to catalyse the CuAAC reaction of **5** and **7**. The guanine moiety seemed to affect the reactivity of the copper(I) catalyst. However, when employing Me_6TREN as the ligand, CuBr was sufficiently protected and remained active to successfully catalyse the CuAAC reaction to yield (30%) a trithiocarbonate RAFT agent with O^6-benzylguanine functionality (**9**). It was shown that this RAFT agent can be used to successfully polymerize *tert*-butyl acrylate with a low dispersity and provide a facile route for the synthesis of a polymer with an α-O^6-benzylguanine chain-end. Furthermore, the *t*-butyl ester groups of the polymer can be deprotected and the polymeric pendant groups further modified.

3.3. Experimental

3.3.1. General details

1-Methylpyrrolidine (≥ 98 %), 2-amino-6-chloropurine (≥ 99 %), 4-aminobenzyl alcohol (98 %), sodium azide (99.5 %), sodium hydride (60 % dispersion in mineral oil), but-3-yn-2-ol (97 %), aluminium oxide (activated, basic), $CuBr_2$ (98 %), Me_6TREN (97 %), DMF (anhydrous 99.8 %), sulphuric acid (95-98 %), methanol, ethyl acetate, dichloromethane, diethyl ether, petroleum ether, and pentane were purchased from Sigma-Aldrich. Anhydrous magnesium sulphate, 4-dimethylaminopyridine (99 %), *n*-butanethiol (> 98 %), 4-toluenesulfonyl chloride (for synthesis), acetic acid (glacial, 100 %) and HCl (32%) were purchased from Merck. PMDETA (99 %) was purchased from Aldrich, sodium nitrite, potassium hydroxide (85 %) from Scienceworld, carbon disulphide (99 %) from LabChem, phenylhydrazine from BDH, sodium ascorbate from Fluka analytical, triphenylphosphine (99 %) from Acros, and $CuSO_4 \cdot 5H_2O$ from Holpro analytics. All were used as received. 2,2-Azobis(isobutyronitrile) (AIBN), from Riedel-de Haën, was recrystallized from methanol and dried under vacuum. $CuBr_2$ was suspended in excess glacial acetic acid, overnight. It was then filtered, washed with ethanol and anhydrous diethyl ether, dried and stored under argon. Distilled deionized water was obtained from a Millipore Milli-Q purification system. *Tert*-butyl acrylate (Sigma, 98 %, 10-20 ppm monomethyl ether hydroquinone as inhibitor) was run through an aluminium oxide column before use. Reactions were monitored by thin layer chromatography using Machery-Nagel Silica gel 60 plates with a UV 254 fluorescent indicator. Silica gel 60 (0.063 – 0.2mm/70 – 230 mesh) was purchased from Machery-Nagel. Moisture- and oxygen-sensitive reactions were carried out under an inert atmosphere by purging with argon.

^{1}H, ^{13}C, COSY, gHSQC and gHMBC NMR spectra were recorded on a Varian-Unity (300-, 400-, or 600 MHz) spectrometer. Samples for NMR were prepared in deuterated solvents – $CDCl_3$ (Sigma, 99.8 %), D_2O (MagniSolv, 99.6 %), DMSO-d_6 (MagniSolv, 99.8 %), acetone-d_6 (MagniSolv, 99.8 %) – with trimethylsilane (TMS) as an internal reference. Abbreviations for NMR data: s = singlet, bs = broad singlet, d = doublet, t = triplet; q = quartet; p = pentet, sex = sextet; dd = doublet of doublets, qt = quartet of doublets, m = multiplet. Mass spectrometry was performed on a Waters Synapt G2 with Electron Spray Ionization (ESI) in the positive mode. SEC samples were run on a Waters SEC instrument comprising of a

Waters 2487 dual wavelength UV detector, a Waters 1515 isocratic pump, Waters 410 differential refractometer (T = 30 °C), Waters 717 plus autosampler, and a Waters in-line degasser. Two PLgel 5 μm mixed-C columns and a PLgel 5 μm guard column with a column temperature of 30 °C were used. The eluent system comprised THF (HPLC grade, BHT stabilized) at a flow rate of 1 $mL \cdot min^{-1}$ at a pressure of 941 psi. Sample concentrations were 2 $mg \cdot mL^{-1}$. Narrow polystyrene standards with molecular weight range of 580 – 318700 $g \cdot mol^{-1}$ were used for calibration. IR spectra were recorded using a Thermo Nicolet iS10 FTIR with a ZnSe ATR attachment and an LC-transform attachment. Spectra were recorded in the range of 500-4000 cm^{-1}. Resolution was set to 8 cm^{-1}, and 64 scans per sample. Omnic spectra software was used for data acquisition and processing.

3.3.2. Synthetic procedures

3.3.2.1. (4-Azidophenyl)methanol (2)

A solution of 4-aminobenzyl alcohol (0.40 g, 3.25 mmol) in acetic acid (1.4 mL) in a 50 mL round bottomed flask containing sulphuric acid (0.14 mL) was cooled to 0 °C. A cold solution of sodium nitrite (0.224 g, 3.25 mmol) in water (1 mL) was added. The resulting mixture was stirred at 0 °C for 5 min. A cold solution of NaN_3 (0.211 g, 3.25 mmol) in water (1 mL) was added dropwise. The reaction mixture was stirred at 0 °C for 30 min. EtOAC (15 mL) and brine (10 mL) were added to the reaction mixture. The organic layer was washed with brine (3 × 10 mL) and 10 % $NaHCO_3$ (3 × 10 mL), dried over anhydrous $MgSO_4$ and concentrated yielding 0.44 g (91 %) pure product as an orange oil. ^{1}H NMR (300 MHz, $CDCl_3$) δ: 7.36 (d, J = 8.5 Hz, 2H), 7.03 (d, J = 8.5 Hz, 2H), 4.66 (s, 2H), 1.76 (bs, 1H).

3.3.2.2. 1-(2-Amino-7H-purin-6-yl)-1-methylpyrrolidin-1-ium chloride (4)

1-(2-amino-7H-purin-6-yl)-1-methylpyrrolidin-1-ium chloride was prepared as reported in literature[32]. 6-Chloropurine-2-amine (0.5 g, 2.95 mmol) was suspended in DMF (10 mL) in a 50 mL round bottomed flask. The mixture was stirred for 30 minutes after which 1-methylpyrrolidine (0.94 mL, 8.85 mmol) was added. After stirring for 2 days, the product was precipitated with acetone and centrifuged. The solid was dried to obtain 0.67 g (89 %)

pure product as a pale-yellow solid. ^{1}H NMR (300 MHz, DMSO-d_6) δ: 13.40 (bs, 1H), 8.34 (s, 1H), 7.10 (s, 2H), 4.60 (m, 2H), 3.97 (m, 2H), 3.65 (s, 3H), 2.24 (m, 2H), 2.06 (m, 2H).

3.3.2.3. 6-((4-Azidobenzyl)oxy-7H-purin-2-amine (5)

(4-Azidophenyl)methanol (0.117 g, 0.79 mmol) in DMF (2 mL) was added to a 50 mL three-necked round bottomed flask under argon. NaH (60 %) (0.056 g, 2.36 mmol of NaH component) was added in 3 portions over 5 min and stirred until the solution turned into a deep purple colour. 1-(2-Amino-7H-purin-6-yl)-1-methylpyrrolidin-1-ium chloride (0.2 g, 0.79 mmol) and DMAP (0.011 g, 0.09 mmol) in DMF (2 mL) was purged with argon and added dropwise. The reaction mixture was stirred for 4 h at room temperature. Water (1 mL) was added to quench all excess NaH and the solvent removed. The product was purified by column chromatography (DCM : MeOH = 95 : 5, R_f = 0.4). The solvent was removed yielding 0.144 g (65 %) of the pure product as a yellow solid. ^{1}H NMR (300 MHz, DMSO-d_6) δ: 12.44 (bs, 1H), 7.82 (s, 1H), 7.57 (d, J = 8.4 Hz, 2H), 7.16 (d, J = 8.4 Hz, 2H), 6.27 (s, 2H), 5.46 (s, 2H). MS (ESI): m/z = 283.1 (calculated 283.3 for $[M + H]^+$).

3.3.2.4. Phenylazide (6)

This compound was prepared as described in literature[18]. A mixture of HCl 32% (6 mL) and water (20 mL) in a 50 mL round bottom flask was cooled to 0 °C. Phenylhydrazine (3 mL, 30.5 mmol) was added dropwise while stirring vigorously. Sodium nitrite (2.5 g, 35.6 mmol) in water (3mL) was added dropwise. After complete addition, the mixture was stirred at 0 °C for 30 minutes. Water was added, the product extracted with diethyl ether (3 × 20 mL), dried with anhydrous $MgSO_4$ and concentrated. The product was purified by column chromatography (pentane, R_f = 0.6). The solvent was removed yielding 0.987 g (28 %) of the pure product as a very pale-yellow oil. We seemed to have lost some product during evaporation of the solvent, and ascribed the low boiling point (49-50 °C) of the product as a possible reason for the low final yield. ^{1}H NMR (400 MHz, $CDCl_3$) δ: 7.36 (t, J = 7.4 Hz, 2H), 7.15 (t, J = 7.3 Hz, 1H), 7.05 (d, J = 8.7 Hz, 2H).

3.3.2.5. Potassium butyl carbonotrithioate

Potassium butyl carbonotrithioate was prepared exactly as in literature[18]. ^{1}H NMR (300 MHz, D_2O-d_6) δ: 3.21 (t, *J* = 7.6 Hz, 2H), 1.66 (p, *J* = 7.4 Hz, 2H), 1.43 (sex, *J* = 7.6 Hz, 2H), 0.92 (t, *J* = 7.4 Hz, 3H).

3.3.2.6. 2-Tosyloxy-3-butyne

But-3-yn-2-ol (1 g, 14.3 mmol), tosyl chloride (3.264 g, 17.1 mmol) and diethyl ether (50 mL) in a 100 mL round bottom flask were cooled to 0 °C. Potassium hydroxide (2 g, 35.7 mmol) was added in small portions over 20 minutes. The suspension was stirred for 3 h. The reaction mixture was filtered, washed with water (3 × 30 mL), dried over anhydrous $MgSO_4$ and concentrated to yield 2.91 g (91 %) of a white crystalline solid. ^{1}H NMR (300 MHz, DMSO-d_6) δ: 7.82 (d, *J* = 8.2 Hz, 2H), 7.48 (d, *J* = 8.2 Hz, 2H), 5.25 (qd, *J* = 6.54, 2.09 Hz, 1H), 3.66 (d, *J* = 2.1 Hz, 1H), 2.42 (s, 3H), 1.43 (d, *J* = 6.6 Hz, 3H).

3.3.2.7. But-3-yn-2-yl butyl carbonotrithioate (7)

A mixture of potassium butyl carbonotrithioate (0.547 g, 2.7 mmol), 2-tosyloxy-3-butyne (0.5 g, 2.2 mmol) and THF (15 mL) in a 50 mL round bottom flask was stirred at room temperature overnight. The reaction mixture was filtered and concentrated. The product was purified by column chromatography (petroleum ether : pentane = 2 : 1, R_f = 0.5). The solvent was removed yielding 0.46 g (95 %) of the pure product as a yellow oil. The product is light sensitive, and can be kept in the freezer for a limited time. ^{1}H NMR (300 MHz, DMSO-d_6) δ: 4.84 (qd, *J* = 6.9, 2.3 Hz, 1H), 3.46 (d, *J* = 2.4 Hz, 1H), 3.40 (t, *J* = 7.1 Hz, 2H), 1.63 (p, *J* = 7.1 Hz, 2H), 1.58 (d, *J*= 7.1 Hz, 3H), 1.38 (sex, *J* = 7.4 Hz, 2H), 0.89 (t, *J* = 7.4 Hz, 3H).

3.3.2.8. Butyl (1-(1-phenyl-1H-1,2,3-triazol-4-yl)ethyl) carbonotrithioate (8)

The CuAAC reaction of **6** and **7** was carried out using three different sources of copper(I).

(a) Phenylazide (218 mg, 1.83 mmol), but-3-yn-2-yl butyl carbonotrithioate (400 mg, 1.83 mmol), $CuSO_4 \cdot 5H_2O$ (45 mg, 0.18 mmol), sodium ascorbate (90 mg, 0.46 mmol) and DMF (1 mL) were added to a microwave vial. The reaction mixture was stirred

overnight. THF (30 mL) was added and the mixture passed through an aluminium oxide plug. The solvent was removed by rotary evaporation and the product purified by column chromatography (ethyl acetate : pentane, 1 : 9, R_f = 0.5). The solvent was removed yielding 0.21 g (34 %) of the product as a dark yellow solid. ^{1}H NMR (300 MHz, DMSO-d_6) δ: 8.89 (s, 1H), 7.90 (d, *J* = 7.5 Hz, 2H), 7.60 (t, *J* = 7.5 Hz, 2H), 7.50 (t, *J* = 7.4 Hz, 1H), 5.51 (q, *J* = 7.0 Hz, 1H), 3.40 (t, *J* = 7.5 Hz, 2H), 1.82 (d, *J* = 7.0 Hz, 3H), 1.64 (p, *J* = 7.3 Hz, 2H), 1.38 (sex, *J* = 7.3 Hz, 2H), 0.89 (t, *J* = 7.3 Hz, 3H).

(b) CuBr (18 mg, 0.13 mmol), PMDETA (27 mg, 0.15 mmol) and DMF (0.5 mL) were added to a microwave vial and purged with argon. Phenylazide (76 mg, 0.64 mmol) and but-3-yn-2-yl butyl carbonotrithioate (140 mg, 0.64 mmol) were separately degassed before being added by a gastight syringe. The reaction mixture was stirred overnight at room temperature. THF (30 mL) was added, and the mixture passed through an aluminium oxide plug. The solvent was removed yielding 0.18 g (83 %) of the product as a dark yellow solid.

(c) $CuBr(PPh_3)_3$ was prepared, as in literature, from the reaction of $CuBr_2$ and PPh_3[33]. $CuBr(PPh_3)_3$ (11 mg, 0.01 mmol), phenylazide (27 mg, 0.23 mmol) and but-3-yn-2-yl butyl carbonotrithioate (50 mg, 0.23 mmol) were added to a microwave vial and stirred overnight at room temperature. The product was dissolved in ethyl acetate (10 mL) and filtered. The solvent was removed and the product isolated. ^{1}H NMR showed a conversion above 90 %, as well as the presence of some impurities. In the case where DMF was used as a solvent conversion was much lower.

3.3.2.9. 1-(1-(4-(((2-amino-7H-purin-6-yl)oxy)methyl)phenyl)-1H-1,2,3-triazol-4-yl)ethyl butyl carbonotrithioate (9)

Cu(I)Br (22 mg, 0.16 mmol), Me_6TREN (57 µL, 0.21 mmol), sodium ascorbate (15 mg, 0.08 mmol) and DMF (0.3 mL) were added to a microwave vial and purged with argon. **8** (150 mg, 0.53 mmol) was dissolved in DMF (0.7 mL) after which but-3-yn-2-yl butyl carbonotrithioate (232 mg, 1.06 mmol) was added. The mixture was degassed separately before being added to the microwave vial with a gastight syringe. The reaction mixture was stirred overnight. The solvent was removed, and the product purified by column chromatography (DCM : MeOH = 95 : 5, R_f = 0.3). The solvent was removed yielding 0.080

g (30 %) of the pure product as a yellow solid. ^{1}H NMR (300 MHz, DMSO-d_6) δ: 12.45 (bs, 1H), 8.90 (s, 1H), 7.90 (d, *J* = 8.6 Hz, 2H), 7.84 (bs, 1H), 7.71 (d, *J* = 8.6 Hz, 2H), 6.31 (bs, 2H), 5.56 (s, 2H), 5.49 (q, *J* = 7.1 Hz, 1H), 3.39 (t, *J* = 7.4 Hz, 2H), 1.79 (d, *J* = 7.1 Hz), 1.63 (p, *J* = 7.4 Hz, 2H), 1.35 (sex, *J* = 7.2 Hz, 2H), 0.88 (t, *J* = 7.2 Hz, 3H). ^{13}C NMR (300 MHz, DMSO-d_6) δ: 222.36, 159.61, 155.26, 147.21, 139.08, 137.93, 137.93, 136.06, 129.81, 129.76, 121.43, 120.04, 119.99, 113.46, 65.90, 41.48, 35.94, 29.60, 21.40, 20.10, 13.39. MS (ESI): *m/z* = 501.13 (calculated 501.66 for $[M+H]^+$).

3.3.2.10. General polymerization procedure for PtBA

Tert-butyl acrylate (0.921 g, 7.2 mmol), **9** (0.040 g, 0.08 mmol), AIBN ($2{,}6 \times 10^{-3}$ g, 0.016 mmol), and DMF (0.22 mL) was added to a 50 mL Schlenk flask. The contents were purged with argon for 15 minutes. The flask was lowered into a 60 °C oil bath. After 4 h the solution was observed to be viscous. The flask was opened to air and an aliquot was removed and dissolved in $CDCl_3$ for ^{1}H NMR analysis. Acetone was added to the polymerization mixture after which the polymer was precipitated twice into a mixture of water and methanol (1 :1). The polymer was redissolved in acetone and dried by rotary evaporation using a water bath at 70 °C. Dissolution in acetone and rotary evaporation was repeated 3 times. The polymer was dried for 24 h under vacuum at 70 °C.

3.4. References

(1) Moad, G.; Rizzardo, E.; Thang, S. H. *Aust. J. Chem.* **2005**, *58* (6), 379–410.

(2) Keddie, D. J.; Moad, G.; Rizzardo, E.; Thang, S. H. *Macromolecules* **2012**, *45* (13), 5321–5342.

(3) Perrier, S.; Takolpuckdee, P.; Westwood, J.; Lewis, D. M. *Macromolecules* **2004**, *37* (8), 2709–2717.

(4) Hill, M. R.; Carmean, R. N.; Sumerlin, B. S. *Macromolecules*. **2015**, *48* (16) 5459–5469.

(5) Hawker, C. J. *Science*. **2005**, *309* (5738), 1200–1205.

(6) Willcock, H.; O'Reilly, R. K. *Polym. Chem.* **2010**, *1* (2), 149–157.

(7) Boyer, C.; Bulmus, V.; Davis, T. P.; Ladmiral, V.; Liu, J.; Perrier, S. *Chem. Rev.* **2009**, *109* (11), 5402–5436.

(8) Perrier, S.; Takolpuckdee, P.; Westwood, J.; Lewis, D. M. *Macromolecules* **2004**, *37* (8), 2709–2717.

(9) Keddie, D. J.; Moad, G.; Rizzardo, E.; Thang, S. H. *Macromolecules*. 2012, pp 5321–5342.

(10) Hong, C. Y.; Pan, C. Y. *Macromolecules* **2006**, *39* (10), 3517–3524.

(11) Johnsson, N.; Johnsson, K. *ChemBioChem* **2003**, *4* (9), 803–810.

(12) Keppler, A.; Kindermann, M.; Gendreizig, S.; Pick, H.; Vogel, H.; Johnsson, K. *Methods* **2004**, *32* (4), 437–444.

(13) Keppler, A.; Gendreizig, S.; Gronemeyer, T.; Pick, H.; Vogel, H.; Johnsson, K. *Nat. Biotechnol.* **2002**, *21* (1), 86–89.

(14) Choudhary, S.; Barth, S.; Verma, R. S. *Mol. Diagnosis Ther.* **2017**, *21* (3), 315–326.

(15) Gronemeyer, T.; Chidley, C.; Juillerat, A.; Heinis, C.; Johnsson, K. *Protein Eng. Des. Sel.* **2006**, *19* (7), 309–316.

(16) Kampmeier, F.; Ribbert, M.; Nachreiner, T.; Dembski, S.; Beaufils, F.; Brecht, A.; Barth, S. *Bioconjug. Chem.* **2009**, *20* (5), 1010–1015.

(17) Kolb, H. C.; Sharpless, K. B. *Drug Discov. Today* **2003**, *8* (24), 1128–1137.

(18) Akeroyd, N.; Pfukwa, R.; Klumperman, B. *Macromolecules* **2009**, *42* (8), 3014–3018.

(19) Balsiger, R. W.; Montgomery, J. A. *J. Org. Chem.* **1960**, *25* (9), 1573–1575.

(20) Seela, F.; Ramzaeva, F.; Rosemeyer. *Science of Synthesis Product class 17: Purines - Bicylclic ring systems each with one or two N-atom.*; Thieme Chemistry, 2003.

(21) Koyama, K.; Hitomi, K.; Terashima, I.; Kohda, K. *Chem. Pharm. Bull. (Tokyo).* **1996**, *44* (7), 1395–1399.

(22) Lembicz, N. K.; Grant, S.; Clegg, W.; Griffin, R. J.; Heath, S. L.; Golding, B. T. *J. Chem. Soc. Trans. 1* **1997**, No. 3, 185–186.

(23) Kindermann, M.; George, N.; Johnsson, N.; Johnsson, K. *J. Am. Chem. Soc.* **2003**, *125* (26), 7810–7811.

(24) Tornøe, C. W.; Christensen, C.; Meldal, M. *J. Org. Chem.* **2002**, *67* (9), 3057–3064.

(25) Chem, A.; Ed, I. *Angew. Chem. Int. Ed.* **2002**, *41* (14), 2596–2599.

(26) Bock, V. D.; Hiemstra, H.; Van Maarseveen, J. H. *Eur. J. Org. Chem.* **2006**, 51–68.

(27) Kolb, H. C.; Finn, M. G.; Sharpless, K. B. *Angew. Chem. Int. Ed.* **2001**, *40* (11), 2004–2021.

(28) Díez-González, S. *Catal. Sci. Technol.* **2011**, *1* (2), 166.

(29) Berg, R.; Straub, B. F. *Beilstein Journal of Organic Chemistry*. **2013**, pp 2715–2750.

(30) Lal, S.; Díez-González, S. *J. Org. Chem.* **2011**, *76* (7), 2367–2373.

(31) Candelon, N.; Lastécouères, D.; Diallo, A. K.; Ruiz Aranzaes, J. *Chem. Commun.* **2008**, *41* (6), 741–743.

(32) Islam, M. M.; Fujii, S.; Sato, S.; Okauchi, T.; Takenaka, S. *Bioorganic Med. Chem.* **2015**, *23* (15), 4769–4776.

(33) Gujadhur, R.; Venkataraman, D.; Kintigh, J. T. *Tetrahedron Lett.* **2001**, *42*, 4791–4793.

Chapter 4: Towards the synthesis of SNAP-tag labels based on metal-chelating polymers.

4.1. Introduction

Biomedical applications of metal-chelating polymers (MCPs) were first explored by Torchilin and coworkers[1–3]. MCPs have binding sites as functionalities in repeating units, which translates into a higher metal-loading capacity and with that an increase in the effectiveness of the metal species. As gadolinium carriers for contrast enhancement in magnetic resonance imaging (MRI), MCPs increased the local Gd^{3+} concentration and with that the quality of images and signal intensity[4]. In radiotherapy, chelating polymers containing large amounts of radioactive metal binding sites were attached to an antibody (Figure 4.1) showing an increase in specific radioactivity[1,2]. The development of reversible deactivation radical polymerization (RDRP), has made it possible to synthesize polymers with controlled molecular weights, low dispersities, and to achieve control over chain-end functionality. These advances have led to the improvement of existing applications, and the development of new applications of metal-chelating polymers in radioimmunotherapy[5–10], cell imaging[11–13], magnetic resonance imaging[14,15] and as optoelectronic materials[16,17].

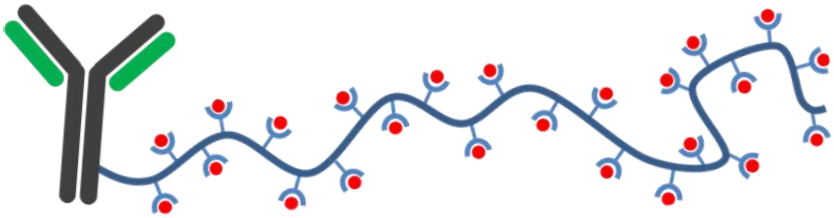

Figure 4.1: Metal-chelating polymer attached to an antibody.

The development of MCPs as elemental tags for mass cytometry[11,12] took advantage of reversible addition fragmentation chain transfer (RAFT) polymerization as a form of RDRP to synthesize MCPs with a low dispersity and chain-end functionality. In this chapter, we report the synthesis of an acrylate-based polymer with an O^6-benzylguanine (BG) α-chain-end functionality and its subsequent modification to carry a chelating-ligand on each repeat

unit. The α-BG functionality enables specific and covalent conjugation to an antibody *via* SNAP-tag. Furthermore, the post-polymerization modification of the ω-trithiocarbonate chain-end is shown by attaching a maleimide functional fluorophore after aminolysis of the trithiocarbonate moiety into a thiol, which can be utilized in further coupling reactions[18–21]. This chapter shows preliminary investigations into the development of MCP-based antibody-tags, which we envision using to develop a spatial cell-imaging technique using SEM-EDS.

4.2. Results and discussion

4.2.1. Steps towards the synthesis of a metal-chelating polymer

The synthesis of the metal-chelating polymer described in this chapter commenced with the synthesis of a poly(*tert*-butyl acrylate) (P*t*BA) backbone, using the O^6-benzylguanine functional RAFT agent (**1** in Scheme 4.1) developed in Chapter 3.

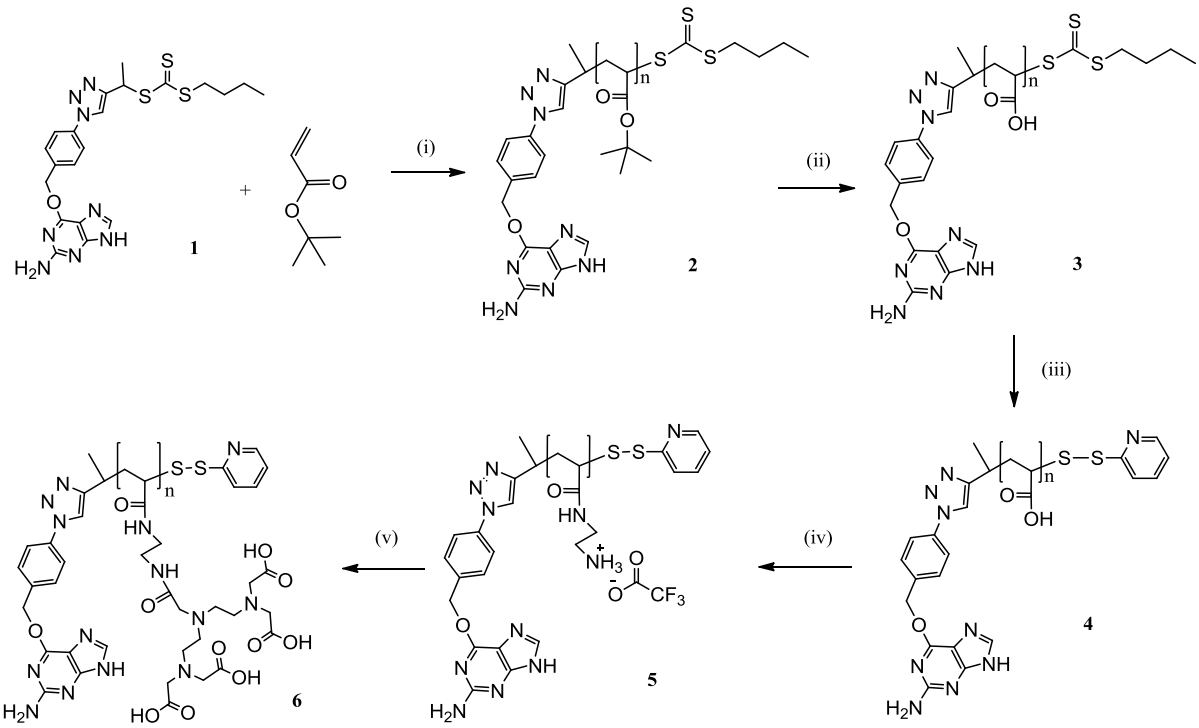

Scheme 4.1: Synthesis of poly(DTPA) (**6**). (i) AIBN, DMF, 5 h, 60 °C. (ii) DCM/TFA (7 : 3), overnight, r.t. (iii) DTP, ethanolamine, acetonitrile, overnight, r.t. (iv) (a) *t*-BOC-ethylenediamine, DMTMM, H_2O, overnight, r.t. (b) DCM/anisole/TFA (6 : 1 : 3), 3 h, r.t. (v) DTPA, NaOH, pH 8.5, DMTMM, 2 h, r.t.

The theoretical number average molecular weight ($M_{n,\,theo}$) can be calculated as a function of conversion:

$$M_{n,theoretical} = \frac{[M]_i}{[CTA]_i} \times \alpha \times M_M + M_{CTA} \qquad \text{(Eq. 4.1)}$$

where $[M]_i$ and $[CTA]_i$ are the initial monomer and CTA concentration, M_M and M_{CTA} are the molar masses of the monomer and the CTA respectively and α is the monomer conversion. Two different molecular weights were targeted and conversions were determined with ^{1}H NMR spectroscopy, using the signals of the vinylic monomer at 6.27, 6.02, and 5.71 ppm and the signal of the methine polymer backbone at 2.15-2.35 ppm. Both polymers were obtained

in almost quantitative yields and the experimental M_n was calculated from ^{1}H NMR end-group analysis. The ratio of the integrated signal of the methylene protons adjacent to the O-atom at 5.70 ppm and the polymer backbone methine between 2.35 and 2.15 ppm was used to determine the experimental degree of polymerization (DP_{NMR}). $M_{n,NMR}$ could then be calculated using Eq. 4.2.

$$M_{n,NMR} = DP_{NMR} \times M_M + M_{CTA} \qquad \text{(Eq. 4.2)}$$

Size exclusion chromatography (SEC) in THF was also carried out to determine the experimental M_n and dispersity ($Đ$). $M_{n,theo}$ and $M_{n,SEC}$ were in good agreement while $M_{n,NMR}$ differed significantly (Table 4.1). The SEC data provides a good indication of the dispersity, however $M_{n,SEC}$ is measured relative to polystyrene standards which may lead to a systematic deviation of the results. While ^{1}H NMR is a more quantitative technique, this also has its limits at high molar masses, due to the small integrals associated with the end-groups.

Table 4.1: Results for the polymerization of two different chain lengths of P*t*BA.

	[RAFT]:[AIBN]:[*t*BA]	$M_{n,th}$ [a]	$M_{n,SEC}$ [b]	DP_{SEC}	$M_{n,NMR}$ [c]	DP_{NMR} [d]	$Đ$
1	1 : 0.2 : 170	22200	21100	165	34000	262	1.13
2	1 : 0.2 : 90	12000	13000	97	21100	161	1.09

[a] *Theoretical molar mass calculated from Eq. 4.1.* [b] $M_{n,SEC}$ *obtained from SEC in THF based on polystyrene standards.* [c] $M_{n,NMR}$ *determined from* ^{1}*H NMR spectroscopy using Eq. 4.2.* [d] *Determined by* ^{1}*H NMR spectroscopy.*

Before carrying out the modification steps towards a metal-chelating polymer (Scheme 4.1), it was essential to confirm the presence of the α-BG end-group. The BG chain-end is essential to our end goal of attaching the functionalized polymer to a protein through SNAP-tag, and its presence was confirmed by the ^{1}H NMR peak of the -O-CH_2- protons (signal *a* in Figure 4.2). The four benzylic protons, the triazole proton, and the proton from the purine are all accounted for in the aromatic region above 7.5 ppm. The presence of the ω-end-group was also confirmed by the peak of the -S-CH_2- protons at 3.44 ppm (*f* in Figure 4.2).

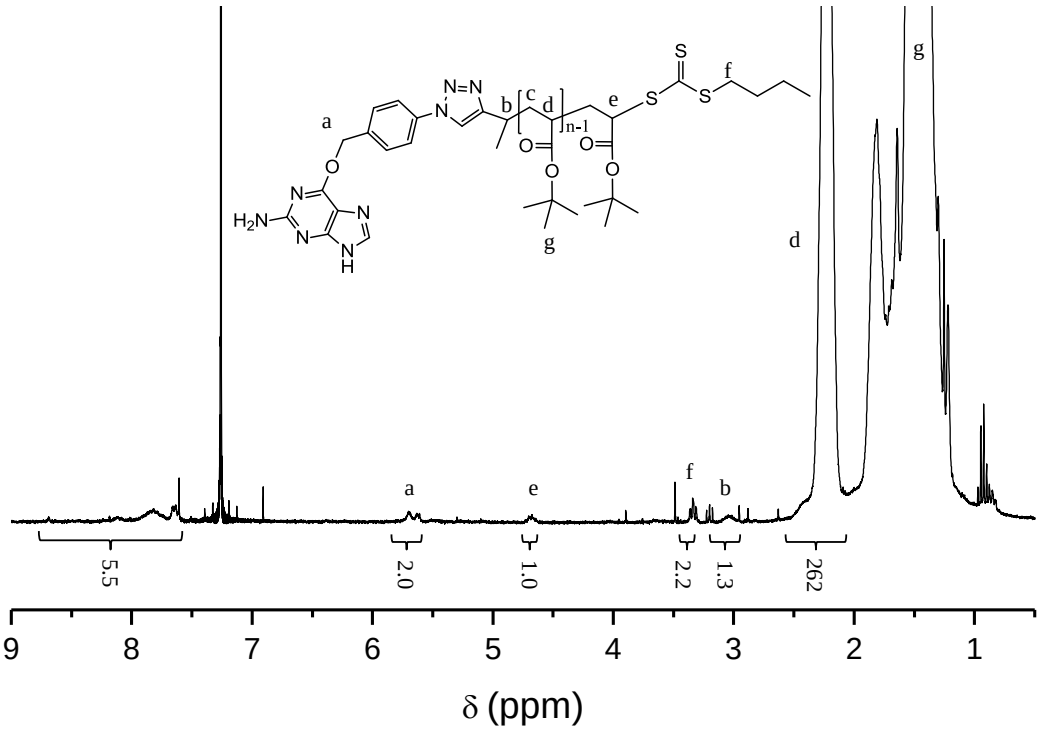

Figure 4.2: ^{1}H NMR ($CDCl_3$) spectrum of P*t*BA with an α-BG chain-end.

The next step in the modification of the polymer (step *iii* in Scheme 4.1) was the hydrolysis of the *t*-butyl acrylate groups to form poly(acrylic acid) (PAA)[22], for the carboxylic acid side chains to become accessible for modification by esterification. ^{1}H NMR showed a drastic decrease in the intensity of the peak corresponding to the 9 *t*-butyl acrylate protons at 1.36 ppm. The ratio of the peak at 1.36 ppm and the polymer backbone methine between 2.7 and 2.2 ppm, indicated that more than 97 % of the repeat units had been deprotected. The presence of the α-end-group was accounted for by signals *a*, *b*, *c*, and *d* in Figure 4.3 and the ω-end-group by signal *g* in Figure 4.3.

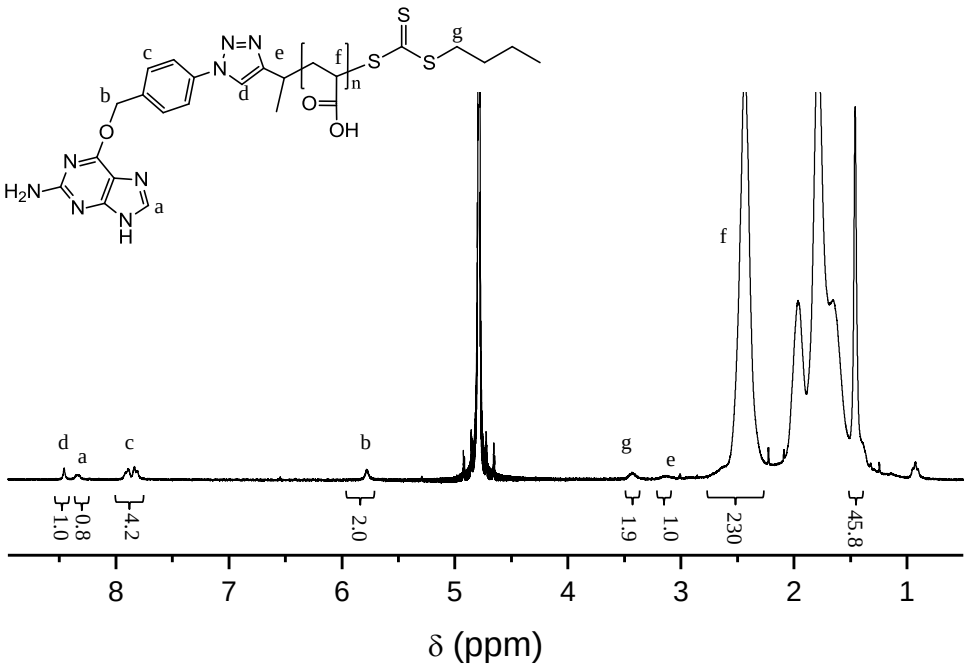

Figure 4.3: ^{1}H NMR spectrum (D_2O) of PAA after the deprotection of the *t*-butyl ester groups of the P*t*BA side chains.

We attempted to protect the ω-chain-end by reducing the trithiocarbonate end group to thiol by reductive aminolysis in the presence of ethanolamine and reacted the thiol with 2,2'-dithiopyridine (DTP) to form a pyridyldisulfide terminated polymer (**4**)[19,23]. We were unable to conclusively determine the degree to which the reaction had proceeded successfully, however the side group functionality remained intact as evidenced by ^{1}H NMR spectroscopy. After attempting to modify the ω-chain-end, we proceeded to functionalize the carboxylic acid side chains by amidation (step *iv a* in Scheme 4.1) with *t*-BOC-ethylenediamine using 4-(4,6-dimethoxy-1,3,5-triazin-2-yl)-4-methylmopholinium chloride (DMTMM) as a coupling agent[24]. The entire sample was used in the following step (step *iv b* in Scheme 4.1) where the BOC (*tert*-butyl carbamate) groups were removed using trifluoroacetic acid (TFA).

^{1}H NMR analysis showed the introduction of the side chain ethylenediamine protons (signal *g* and *h* in Figure 4.4) confirming the synthesis of the amino polymer, and serving to confirm that the preceding reaction (which had not been characterized) had been successful. Comparing the ratio of the integrated ^{1}H NMR peaks at 3.7-2.9 ppm corresponding to the side chain ethylenediamine groups (signal *g* and *h* in Figure 4.4) with that of the signals at 2.4-1.2 ppm corresponding to the polymer backbone protons indicated a high degree of side chain functionalization. There was also no dominant peak around 1.4 ppm, which indicated

that the BOC deprotection (step *iii b* in Scheme 4.1) had been successful. Finally, the ^{1}H NMR spectrum does not seem to support the presence of the pyridyldisulphide ω-chain-end, and signal *i* at 0.91 ppm corresponds to the -C*H*$_3$ signal of the Z group of the RAFT agent *n*-butyl moiety. For our application in SNAP-tag it was far more important to confirm that the α-BG chain-end had remained intact, and this was confirmed by peaks *a*, *b*, *c*, and *d* in Figure 4.4.

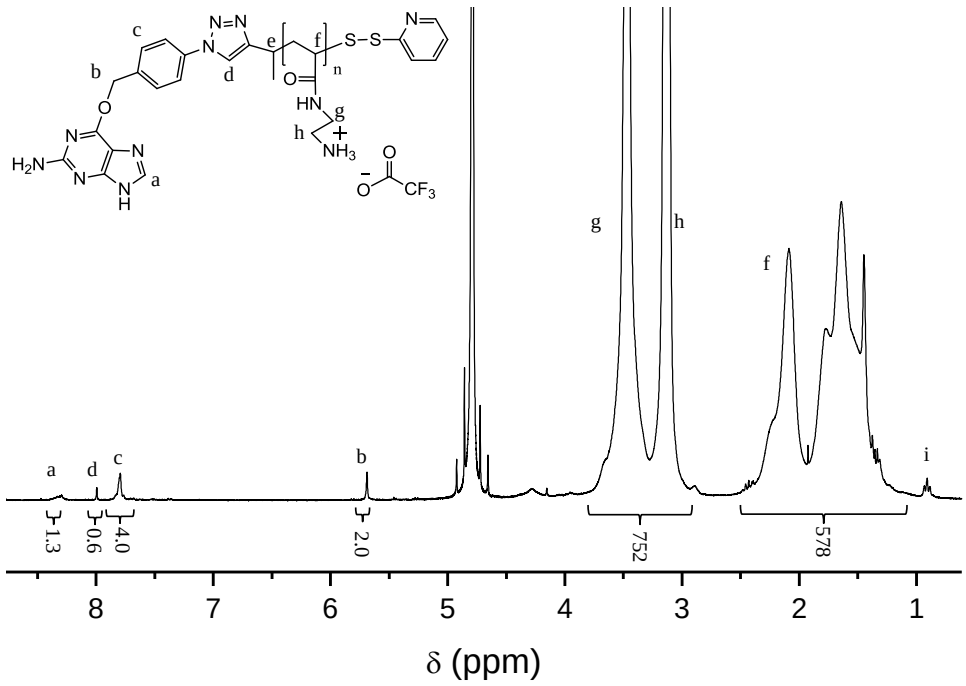

Figure 4.4: ^{1}H NMR spectrum (D_2O) of poly(2-aminoethyl acrylamide).

Finally, DTPA was introduced (step *v* in Scheme 4.1) as the chelating-ligand using DMTMM as a coupling agent. The ^{1}H NMR spectrum was dominated by peaks corresponding to the ligand (Figure 4.5) and signals of the backbone protons dwarfed in comparison. We attributed this to the greater number of protons on the pendant groups compared to the backbone. The high density of the ligand restricts mobility and this leads to peak broadening of the small backbone peaks – making them even more difficult to detect. The suppression of backbone proton peaks was similarly observed by Wang[25] in the synthesis of polythiophene-based molecular brushes and we took this to favourably indicate that we had inserted a high density of ligands on the backbone. The presence of the BG end-group was confirmed in the previous step and we assumed that this had remained intact.

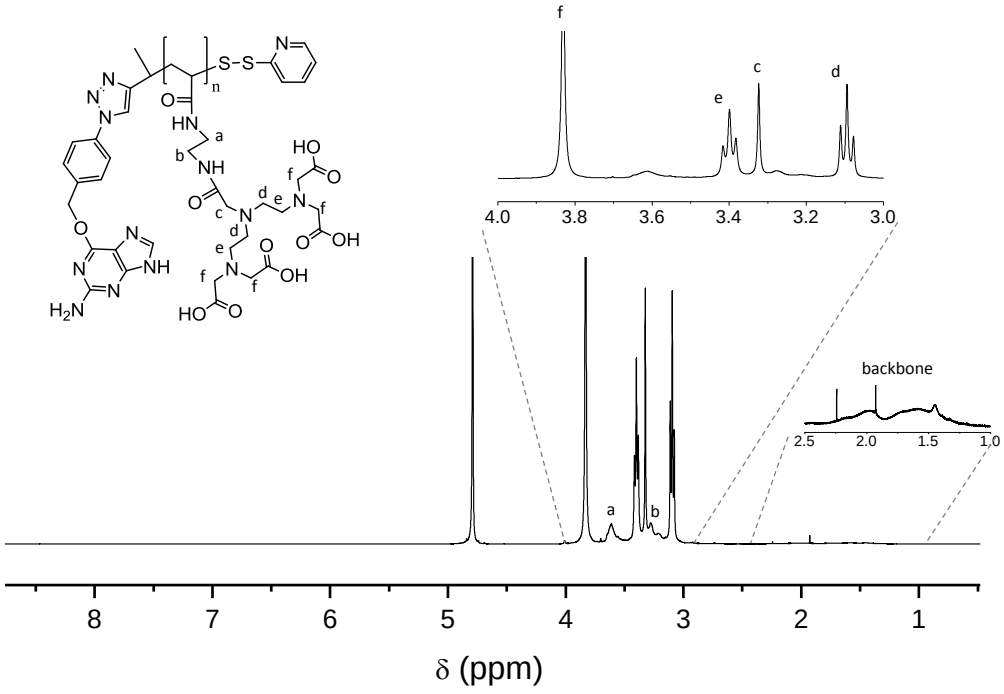

Figure 4.5: ^{1}H NMR spectrum (D_2O) of P(DTPA).

4.2.2. Modifying the ω-chain-end with a fluorophore

Another possibility in the synthesis of SNAP-tag labels using our BG-functional RAFT agent is adding ω-chain-end functionality by post-polymerization modification. RAFT-synthesized polymers contain a thiocarbonyl thio end-group, and this moiety can be converted to a thiol through aminolysis by primary or secondary amines[18,19,21]. The thiol can then be utilized in a further coupling reaction such as disulphide formation or Michael addition[18,26]. Nakayama and Okano took advantage of thiocarbonyl thio end-groups to modify block copolymers to be pyrene-ω-end-labelled in a one-pot procedure[28,29]. In an investigation into aminolysis of RAFT polymers and the simultaneous thiol-ene reactions, Boyer successfully used a solution of hexylamine, for aminolysis, and triethylamine, to deprotonate the thiol, for the subsequent attachment of maleimide-modified biotin to the ω-chain-end of a polymer in a one-pot reaction[21].

The attachment of *N*-(1-pyrene)maleimide has been reported as an effective way to attach a fluorescent dye to a RAFT generated polymer[27,29]. We successfully synthesized a similar maleimide-functional fluorescent probe based on 1,8-naphthalic anhydride (Scheme 4.2). ^{1}H

NMR and FTIR analysis confirmed the synthesis (**8** in Scheme 4.2) after recrystallization from benzene.

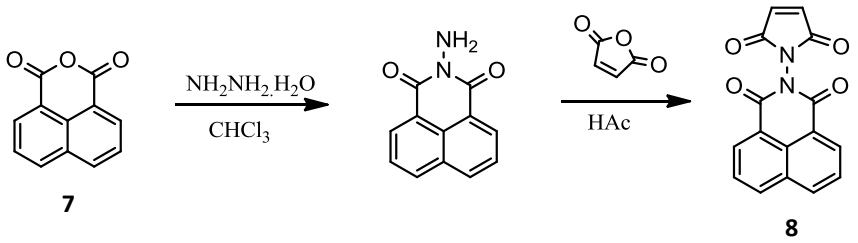

Scheme 4.2: Synthesis of a fluorescent probe based on 1,8-naphthalic anhydride.

We subsequently attempted to attach this probe (**8**) to ω-chain-end of the P*t*BA (**1**). The reaction was carried out with a ratio of [trithiocarbonate] : [maleimide] : [hexylamine] : [triethylamine] of 1 : 5 : 6 : 6. In our envisioned strategy (Scheme 4.3), the ω-trithiocarbonate chain-end of P*t*BA (**2**) would undergo aminolysis to a thiol, followed by a click-type thiol-Michael addition of the maleimide functional dye (**8**). The aromatic region of the ^{1}H NMR spectrum seemed to indicate that the dye had attached to the polymer, however it also indicated the presence of excess dye. The excess hydrophobic dye could potentially be removed with dialysis, however this could also be achieved after the subsequent deprotection of the *t*-butyl ester side chains.

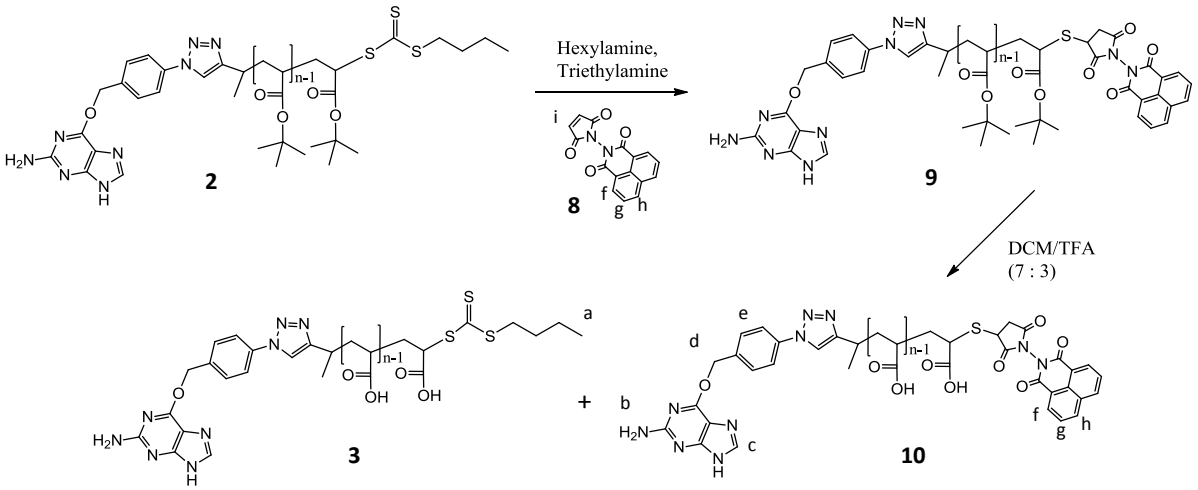

Scheme 4.3: The attachment of a maleimide-functional fluorescent dye (**8**) to P*t*BA (**2**) and the subsequent deprotection of the butyl acrylate side chains to produce a mixture of the ω-fluorescent-functionalized- (**10**) and ω-trithiocarbonate PAA (**3**).

We commenced with the deprotection of the *t*-butyl ester groups, for the two-fold purpose of unveiling the carboxylic acid functionalities of the side chains for further functionalization, and making the polymer water-soluble in order to test the SNAP-tag conjugation in aqueous medium. Analysis by ^{1}H NMR spectroscopy (Figure 4.6) indicated the presence of the ω-trithiocarbonate *n*-butyl -C*H*$_3$ moiety (signal *a*). Relative integration of the -C*H*$_3$ signal (*a*) at 0.85 ppm and the -O-C*H*$_2$- signal (*d*) at 5.56 ppm from the α-BG chain-end showed that about 60 % of the original ω-chain-end was still present. The aromatic region of the ^{1}H NMR spectrum indicated some evidence of the attachment of the dye, however this was hard to quantify due to spectral overlap of the peaks attributable to the dye and the α-chain-end around 8.6 and 7.9 ppm. Peaks *b, c, d,* and *e* in Figure 4.6 allowed us to unequivocally confirm the presence of the α-BG chain-end.

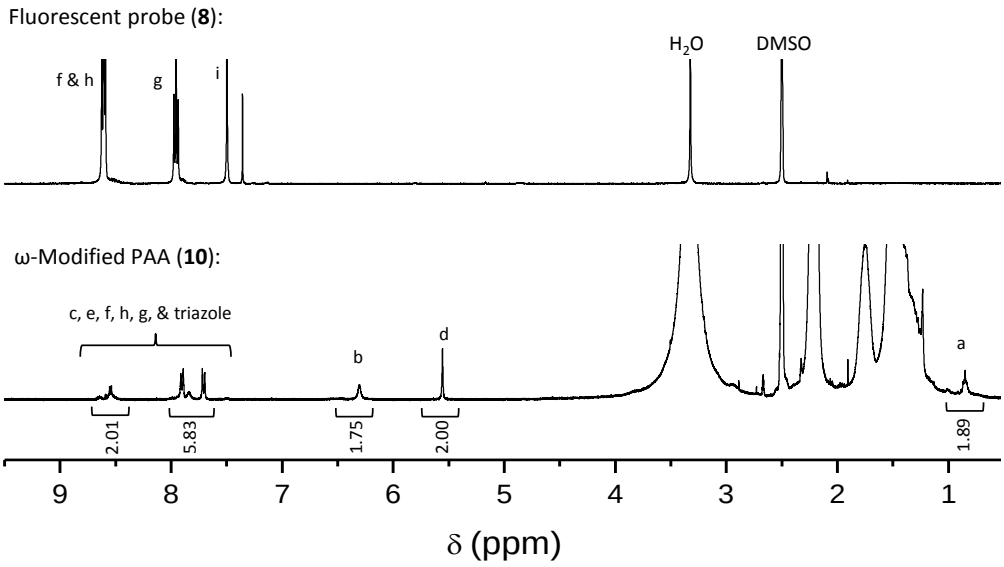

Figure 4.6: ^{1}H NMR spectrum (DMSO-d_6) of maleimide-functional fluorescent probe (**8**) and a mixture of the ω-fluorescent-functionalized PAA (**10**) and the ω-trithiocarbonate PAA (**3**). See Scheme 4.3 for assignments.

UV-vis spectroscopy (Figure 4.7) seemed to provide further evidence that the fluorescent probe had indeed attached to the ω-chain-end of the polymer. An absorbance for **10** was detected with a similar shape as the absorbance of **8** (between 330 and 370 nm). The UV absorption of the amino polymer (**4**) indicates that a polymer which has not undergone ω-modification does not show the UV absorption attributable to the fluorescent probe (**8**).

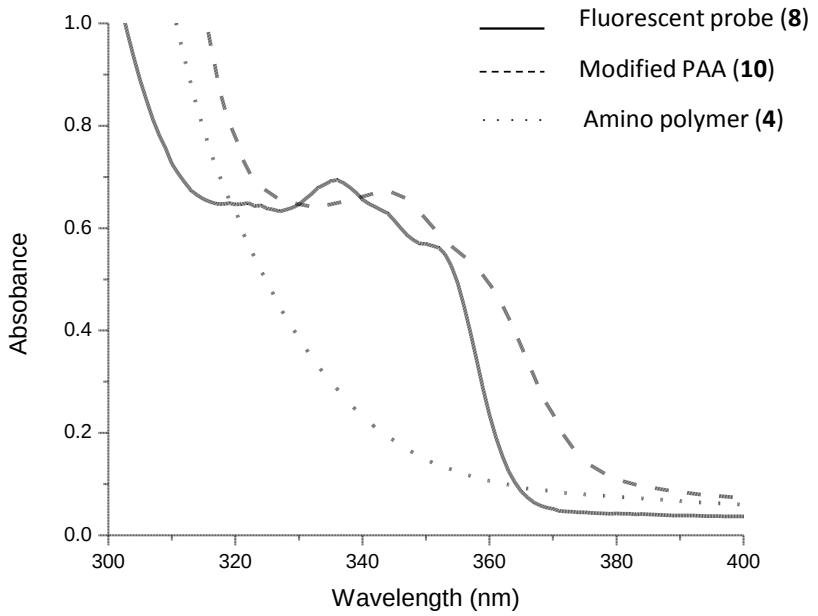

Figure 4.7: UV spectrum showing the possible attachment of the fluorescent probe (**8**) to the ω-chain-end of the polymer.

We have shown that the ω-chain-end of α-BG functional P*t*BA can be modified post-polymerization by aminolysis of the ω-trithiocarbonate and the subsequent thiol-Michael addition click reaction, without affecting the α-BG functionality. Considering the integration of peak *a* in Figure 4.6, we have only achieved around a 40 % conversion of the ω-chain-end, but we hope to improve on this in the near future, as a full conversion would be necessary for certain applications.

4.3. Conclusion

We report the synthesis of a polymer with the potential to metal-chelate. The polymer is based on a polyacrylate backbone with DTPA ligands attached to each of the repeat units and an α-O^6-benzylguanine chain-end. We started with the synthesis of poly(*tert*-butyl acrylate) with an α-BG chain-end, and a low dispersity, using a novel RAFT agent we had designed. The number average molecular weight and end-group content were determined by ^{1}H NMR. Subsequent side-chain modifications were carried out with good yields and without affecting the α-BG functionality of the polymer. Furthermore, we conducted preliminary experiments to functionalize the ω-chain-end of P*t*BA with a maleimide functionalized 1,8-naphthalic anhydride fluorescent probe with positive results. Available literature provides several routes for the post polymerization modification of RAFT-generated polymers [19,21,27–30] and we aim to soon carry out this reaction with a larger conversion. One of the beauties of SNAP-tag technology lies in its specificity towards substrates containing the BG moiety – of which we have confirmed the presence. This chapter seems to pave the way towards an exceptionally versatile new technique for the synthesis of polymeric SNAP-tag labels.

4.4. Experimental

4.4.1. General details

Trifluoroacetic acid (≥ 99 %), di-*tert*-butyl dicarbonate (≥ 99 %), 2,2'-dithiopyridine (Aldrithiol™-2, 98 %), ethanolamine (≥ 99 %), 4-(4,6-Dimethoxy-1,3,5-triazin-2-yl)-4-methylmopholinium chloride (> 96 %), Diethylenetriaminepentaacetic acid (≥ 99 %), 1,88-naphthalic anhydride, triethylamine (>99 %), methanol, dichloromethane, diethyl ether, and acetonitrile (> 99.9 % HPLC reagent grade) were purchased from Sigma-Aldrich. Anhydrous magnesium sulphate, ethylenediamine, sodium carbonate (98 %), and anisole (> 99 %) were purchased from Merck. *n*-Hexylamine (99 %), was purchased from Acros, and hydrazine hydrate (>99 %) from Fluka. All were used as received. 2,2-Azobis(isobutyronitrile) (AIBN), from Riedel-de Haën, was recrystallized from methanol and dried under vacuum. Distilled deionized water was obtained from a Millipore Milli-Q purification system. *Tert*-butyl acrylate (Sigma, 98 %, 10-20 ppm monomethyl ether hydroquinone as inhibitor) was run through an aluminium oxide column before use. Moisture and oxygen sensitive reaction were carried out under an inert atmosphere. Benzoylated dialysis tubing (MWCO 2 kDA, avg flat width 9 mm) was purchased from Sigma-Aldrich. SnakeSkin dialysis tubing (MWCO 3.5 kDA, 35 mm I.D.) was purchased from Thermo Fischer Scientific.

^{1}H NMR spectra were recorded on a Varian-Unity (300-, 400-, or 600 MHz) spectrometer. Samples for NMR were prepared in deuterated solvents – $CDCl_3$ (Sigma, 99.8 %), D_2O (MagniSolv, 99.6 %) – with trimethylsilane (TMS) as an internal reference. Abbreviations for NMR data: s = singlet; d = doublet; t = triplet; bs = broad singlet; bd = broad doublet; bt = broad triplet; q = quartet; m = multiplet. SEC samples were run on a Waters SEC instrument comprising of a Waters 2487 dual wavelength UV detector, a Waters 1515 isocratic pump, Waters 410 differential refractometer (T = 30 °C), Waters 717 plus autosampler, and a Waters in-line degasser. Two PLgel 5 µm mixed-C columns and a PLgel 5 µm guard column with a column temperature of 30 °C. The eluent system comprised THF (HPLC grade, BHT stabilized) at a flow rate of 1 mL.min^{-1} at a pressure of 941 psi. Sample concentrations were 2 mg·mL^{-1}. Narrow polystyrene standards with molecular weight range of 580 – 318700 g·mol^{-1} were used for calibration.

4.4.2. Synthetic procedures

The synthesis of poly(*tert*-butyl acrylate) (shown in Chapter 3) and subsequent modifications were based on the procedure in literature[12].

*4.4.2.1. Deprotection of poly(*tert*-butyl acrylate) to poly(acrylic acid)(3)*

P*t*BA (200 mg) was dissolved in DCM (3 mL) in a 50 mL round-bottomed flask. Trifluoroacetic acid (0.6 mL, 3.6 mmol) was added and the solution was stirred overnight. The polymer precipitated out of solution. The precipitate was collected by filtration and washed first with DCM (30 mL), then with diethyl ether (30 mL). The precipitate was transferred to a round-bottom flask and dried at room temperature on a rotary evaporator for 30 minutes. The polymer was dissolved in H_2O : MeOH (2 : 1) and then dialyzed (MWCO 2 kDA) against water for 3 days. The solution was freeze-dried to yield PAA. ^{1}H NMR (300 MHz, D_2O) δ (ppm): 8.46 (s, 1H), 8.35 (bs, 1H), 7.84 (bd, 4H), 5.78 (bs, 2H), 3.44 (bs, 2H), 3.14 (bs, 1H), 2.7-2.2 (b, 1H per monomer, integration = 230), 2.1-1.3 (b, 2H per monomer), 1.49-1.41 (s, 9H, 2.2 % unremoved *t*-butyl ester), 0.93 (bt, 3H).

4.4.2.2. Synthesis of t-BOC-ethylenediamine

A solution of di-*tert*-butyl dicarbonate (3 g, 13.7 mmol) in DCM (200 mL) was added dropwise to a solution of ethylenediamine (4.9 g, 81.8 mmol) in DCM (50 mL) over 6 h. The reaction mixture was stirred for a further 24 h at room temperature. After the solvent was removed, the oily residue was dissolved in aqueous sodium carbonate (2 M, 100 mL) and extracted with DCM (2 × 200 mL). The organic layer was dried with anhydrous $MgSO_4$ and the solvent removed to yield 1-(*tert*-butyloxycarbonyl)ethyldiamine. ^{1}H NMR (300 MHz, $CDCl_3$) δ (ppm): 4.97 (bs, 1H), 3.12 (q, J = 5.7 Hz, 2H), 2.76 (t, J = 5.7 Hz, 2H), 1.41 (bs, 9H), 1.25 (bs, 2H).

4.4.2.3. ω-Chain-end protection (4)

PAA (140 mg, 0.01 mmol), DTP (52 mg, 0.24 mmol) and acetonitrile (2 mL) were added to a 50 mL Schlenk flask and three freeze-pump-thaw cycles performed, backfilling with argon. Ethanolamine (7.2 mg, 0.12 mmol) in acetonitrile (0.5 mL) was degassed separately and added before the final freeze-pump-thaw cycle. The reaction was stirred overnight at room

temperature. The polymer was precipitated in diethyl ether, dissolved in H_2O and dialyzed (MWCO 2 kDA) against water for 2 days. The solution was freeze-dried to yield pyridyldisulfide terminated PAA.

4.4.2.4. Coupling of t-BOC-ethylenediamine to poly(acrylic acid)

A portion of the PAA (50 mg, 0.004 mmol) was dissolved in H_2O (5 mL) and added to a 50 mL round-bottomed flask. A solution of t-BOC-ethylenediamine (267 mg, 1.67 mmol) in H_2O (5 mL) was added to the polymer solution, immediately followed by a solution of DMTMM (461 mg, 1.67 mmol) in H_2O (8 mL). The mixture was stirred overnight at room temperature. A precipitate formed, the liquid was poured off and the polymer rinsed with H_2O (3 × 10 mL). The polymer was then dissolved in DCM and the solvent removed with a rotary evaporator at room temperature. To azeotropically remove all the water, the dissolution in DCM and rotary evaporation was repeated seven times. The polymer product was used directly in the deprotection step.

4.4.2.5. Deprotection of BOC groups to yield poly(2-aminoethyl acrylamide) (5)

The BOC-protected polymer (entire sample, 90 mg, 0.003 mmol) was dissolved in DCM (9 mL) in a 50 mL round-bottomed flask. Anisole (1.5 mL) and TFA (4.5 mL, 58.8 mmol) was added and the mixture stirred. A transparent precipitate formed on the flask wall. After 3 h the mother liquid was poured off and the precipitate rinsed with diethyl ether (2 × 10 mL). The product was dried by a rotary evaporator at room temperature. The polymer was dissolved in H_2O and then dialyzed (MWCO 3 kDA) against water for 2 days. The solution was freeze-dried to yield the amino polymer as the trifluoroacetate salt. ^{1}H NMR (300 MHz, D_2O) δ (ppm, integrated peak areas are based on the methylene protons adjacent to the O-atom, integration = 2): 8.30 (bs, 1H), 7.99 (s, 1H), 7.79 (bs, 4H), 5.69 (s, 2H), 3.7-3.3 (bs, 2H per monomer), 3.3-3.0 (bs, 2H per monomer), 2.35-1.25 (m, 3H per monomer), 0.91 (bt, 3H).

4.4.2.6. Synthesis of P(DTPA) (6)

DTPA (3.4 g, 80 equivalent to each polymeric repeat unit) and H_2O (5 mL) was added to a 100 mL round-bottomed flask. NaOH (5 M aqueous) was added to dissolve the DTPA and

bring the solution pH to 8.5. DMTMM (239 mg, 8 equivalent to each polymeric repeat unit) was dissolved in H_2O (5 mL) and added to the round-bottomed flask. The mixture was given 5 minutes to pre-react. A solution of poly(2-aminoethyl acrylamide) (25 mg, 0.001 mmol) in H_2O (5 mL) was added. The reaction was stirred for 2 h and then dialyzed (MWCO 3 kDa) against water for 3 days. The solution was freeze-dried to yield poly(DTPA) as a white powder.

4.4.2.7. Synthesis of maleimide-functional 1,8-naphthalic anhydride-based fluorescent probe (8)

1,8-Naphthalic anhydride (500 mg, 2.5 mmol) was stirred in chloroform (40 mL) for 5 minutes. Hydrazine hydrate (0.16 mL, 5 mmol) was added and reaction mixture was stirred under reflux for 4 hour. After cooling, a yellow solid was separated by filtration and dried in a vacuum oven at 100 °C. The product was used directly in the next step. A mixture of the product (430 mg, 2.03 mmol) and maleic anhydride (218 mg, 2.23 mmol) in glacial acetic acid (15 mL) was stirred under reflux for 4 hours. After cooling, a yellow solid obtained by filtration and washed with Na_2CO_3. Recrystallization from benzene yielded (55 mg, 9.3 %) the pure product as a pale yellow powder. ^{1}H NMR (300 MHz, $CDCl_3$) δ (ppm): 8.63 (d, J = 7.5 Hz, 2H), 8.30 (d, J = 8.3 Hz, 2H), 7.81 (t, J = 7.5 Hz, 2H), 6.98 (s, 2H).

*4.4.2.8. Attachment of fluorescent probe to the ω-chain-end of poly(***tert***-butyl acrylate) (9)*

A mixture of P*t*BA (100 mg, 0.005 mmol) and maleimide-functional fluorescent probe, **8**, (7 mg, 0.024 mmol) in DMF (3 mL) in a microwave vial was purged with argon. A solution of *n*-hexylamine (64 mg, 0.032 mmol) and triethylamine (64 mg, 0.032 mmol) in DMF (1 mL) was prepared and purged with argon. A portion of this solution (0.1 mL) was added to the reaction mixture and it was stirred overnight. The reaction mixture was added to a H_2O : MeOH (1 : 1) solution and dialyzed (MWCO 2 kDA) against water for 1 day. The solution was freeze dried to yield ω-modified P*t*BA.

4.4.2.9. Deprotection of ω-modified PtBA to PAA(10)

The reaction was carried out in the same way as 4.4.2.1.

4.5. References

(1) Torchilin, V. P.; Klibanov, A. L.; Slinkin, M. A.; Danilov, S. M.; Levitsky, D. O.; Khaw, B. A. *J. Control. Release*, **1990**, *11* (1989), 297–303.

(2) Torchilin, V. P.; Trubetskoy, V. S.; Narula, J.; Khaw, B. A.; Klibanov, A. L.; Slinkin, M. A. *J. Control. Release* **1993**, *24* (1–3), 111–118.

(3) Torchilin, V. P. *Bioconjug. Chem.* **1999**, *10* (1), 146–149.

(4) Erdogan, S.; Roby, A.; Sawant, R.; Hurley, J.; Torchilin, V. P. *J. Liposome Res.* **2006**, *16* (1), 45–55.

(5) Lu, Y.; Chau, K.; Boyle, A.; Liu, P.; Niehoff, A.; Weinrich, D. *Biomacromolecules* **2012**, *13* (5), 1–15.

(6) Liu, P.; Boyle, A. J.; Lu, Y.; Reilly, R. M.; Winnik, M. A. *Biomacromolecules* **2012**, *13* (9), 2831–2842.

(7) Boyle, A. J.; Liu, P.; Lu, Y.; Weinrich, D.; Scollard, D. A.; Ngo Njock Mbong, G.; Winnik, M. A.; Reilly, R. M. *Pharm. Res.* **2013**, *30* (1), 104–116.

(8) Liu, P.; Cai, Z.; Kang, J. W.; Boyle, A. J.; Adams, J.; Lu, Y.; Mbong, G. N. N.; Sidhu, S.; Reilly, R. M.; Winnik, M. A. *Biomacromolecules* **2014**, *15* (3), 715–725.

(9) Liu, P.; Boyle, A. J.; Lu, Y.; Adams, J.; Chi, Y.; Reilly, R. M.; Winnik, M. A. *Biomacromolecules* **2015**, *16* (11), 3613–3623.

(10) Ngo Ndjock Mbong, G.; Lu, Y.; Chan, C.; Cai, Z.; Liu, P.; Boyle, A. J.; Winnik, M. A.; Reilly, R. M. *Mol. Pharm.* **2015**, *12* (6), 1951–1960.

(11) Lou, X.; Zhang, G.; Herrera, I.; Kinach, R.; Ornatsky, O.; Baranov, V.; Nitz, M.; Winnik, M. A. *Angew. Chemie - Int. Ed.* **2007**, *46* (32), 6111–6114.

(12) Majonis, D.; Herrera, I.; Ornatsky, O.; Schulze, M.; Lou, X.; Soleimani, M.; Nitz, M.; Winnik, M. A. *Anal. Chem.* **2010**, *82* (21), 8961–8969.

(13) Majonis, D.; Ornatsky, O.; Kinach, R.; Winnik, M. A. *Biomacromolecules* **2011**, *12* (11), 3997–4010.

(14) Ladd, D. L.; Hollister, R.; Peng, X.; Wei, D.; Wu, G.; Delecki, D.; Snow, R. A.; Toner, J. L.; Kellar, K.; Eck, J.; Desai, V. C.; Raymond, G.; Kinter, L. B.; Desser, T. S.; Rubin, D. L. *Bioconjug Chem* **1999**, *10* (3), 361–370.

(15) Darras, V.; Nelea, M.; Winnik, F. M.; Buschmann, M. D. *Carbohydr. Polym.* **2010**, *80* (4), 1137–1146.

(16) Shunmugam, R.; Tew, G. N. *J. Am. Chem. Soc.* **2005**, *127* (39), 13567–13572.

(17) Shunmugam, R.; Gabriel, G. J.; Smith, C. E.; Aamer, K. A.; Tew, G. N. *Chem. Eur. J.* **2008**, *14* (13), 3904–3907.

(18) Willcock, H.; O'Reilly, R. K. *Polym. Chem.* **2010**, *1* (2), 149–157.

(19) Boyer, C.; Bulmus, V.; Davis, T. P.; Ladmiral, V.; Liu, J.; Perrier, S. *Chem. Rev.* **2009**, *109* (11), 5402–5436.

(20) Keddie, D. J.; Moad, G.; Rizzardo, E.; Thang, S. H. *Macromolecules* **2012**, *45* (13), 5321–5342.

(21) Boyer, C.; Bulmus, V.; Davis, T. P. *Macromol. Rapid Commun.* **2009**, *30* (7), 493–497.

(22) Mori, H.; Seng, D. C.; Lechner, H.; Zhang, M.; Müller, A. H. E. *Macromolecules* **2002**, *35* (25), 9270–9281.

(23) Shi, H.; Liu, L.; Wang, X.; Li, J. *Polym. Chem.* **2012**, *3* (5), 1182.

(24) Thompson, K.; Michielsen, S. *J. Polym. Sci. Part A Polym. Chem.* **2006**, *44* (1), 126–136.

(25) Wang, M.; Zou, S.; Guerin, G.; Shen, L.; Deng, K.; Jones, M.; Walker, G. C.; Scholes, G. D.; Winnik, M. A. *Macromolecules* **2008**, *41*, 1–6.

(26) Nair, D. P.; Podgórski, M.; Chatani, S.; Gong, T.; Xi, W.; Fenoli, C. R.; Bowman, C. N. *Chem. Mater.* **2014**, *26* (1), 724–744.

(27) Scales, C. W.; Convertine, A. J.; McCormick, C. L. *Biomacromolecules* **2006**, *7* (5), 1389–1392.

(28) Beija, M.; Charreyre, M. T.; Martinho, J. M. G. *Prog. Polym. Sci.* **2011**, *36* (4), 568–602.

(29) Nakayama, M.; Okano, T. *Biomacromolecules* **2005**, *6* (4), 2320–2327.

(30) Keddie, D. J.; Moad, G.; Rizzardo, E.; Thang, S. H. *Macromolecules*. 2012, *45* (13), 5321–5342.

Chapter 5: Epilogue

5.1. Introduction

The goal of this study was to develop a multi-epitope cell-imaging technique assisted by metal-chelating polymers and SEM-EDS. To achieve this we developed a trithiocarbonate RAFT agent with O^6-benzylguanine (BG) functionality, providing a facile route towards the synthesis of α-BG functional polymers. This was followed by modifications towards a metal-chelating polymer (MCP). The α-BG functionality should facilitate polymer-antibody conjugation, and these polymeric antibody labels be utilized to investigate the cell-imaging resolution obtainable with SEM-EDS.

In Chapter 3, we showed the successful synthesis a novel trithiocarbonate RAFT agent with BG functionality on the R-group. This was achieved through CuAAC reaction of but-3-yn-2-yl carbonotrithioate and an O^6-(*p*-azidobenzyl)guanine derivative (developed based on literature[1]) using CuBr as the catalyst and Me_6TREN as a protecting ligand. Synthesis of the BG functional RAFT agent (yield of 30 %) was confirmed with ^{1}H NMR, COSY, gHSQC, gHMBC and ^{13}C NMR as well as MS. Some optimization of the reaction was done to achieve improved yield; however there is still room for improvement. The BG functional RAFT agent was used in the synthesis of poly(*tert*-butyl acrylate) showing good control and a low dispersity. We used ^{1}H NMR analysis to confirm the α-BG end functionality of the polymer.

Chapter 4 started by describing the synthesis of α-BG functional poly(*tert*-butyl acrylate), followed by a series of side-chain modifications, whilst retaining the α-BG chain-end. The first step was the deprotection of the butyl ester group to form poly(acrylic acid) (PAA), followed by a coupling reaction with *t*-BOC-ethylenediamine and the subsequent deprotection of the BOC groups to yield an amine-functional polymer. It was determined by ^{1}H NMR spectroscopy that modification of the repeat units with ethylenediamine was successful. The final step was the attachment of the DTPA ligand to each repeat unit to for α-BG functional poly(DTPA), and this was confirmed by ^{1}H NMR analysis. DTPA in known to be a very efficient chelating ligand[2–4], especially for the lanthanides. Finally, we briefly investigated the ω-chain-end modification by attaching a maleimide functional fluorescent

dye after aminolysis of the ω-trithiocarbonate. Analysis by UV-vis spectroscopy and ^{1}H NMR indicated that the dye was attached to the ω-chain-end; however optimization of this procedure is certainly required in the near future.

5.2. Outlook

In the immediate future we aim to complete the initial goal of our project by using α-BG and ω-fluorescently labelled MCPs to develop a multi-epitope cell-imaging technique using electron microscopy. In addition to this microscopic imaging technique, we aim to further explore diagnostic and therapeutic applications of polymeric metal chelates, chain-end modified with highly specific targeting ligands, such as antibodies.

Ultimately, the RAFT agent developed in Chapter 3 provides a highly versatile route to the synthesis of SNAP-tag labels (Figure 5.1). RAFT polymerization offers control over the chain length and architecture of various polymerizable monomers. We have also shown that the pendant groups of these polymers can be modified post-polymerization without affecting the BG functionality. Post-polymerization modification of the ω-chain-end further increases the versatility of synthesizable labels. Finally, the α-BG chain-end provided by the R-group of the RAFT agent allows conjugation to any SNAP-tag fusion protein.

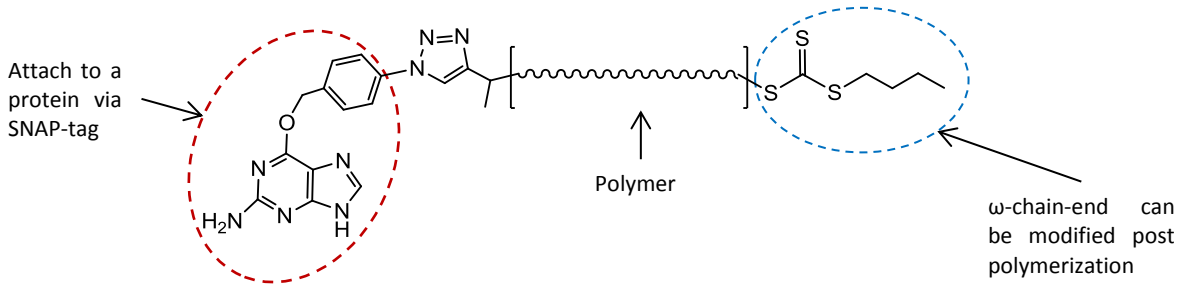

Figure 5.1: General structure of a polymer synthesized using the O^6-benzylguanine functional RAFT agent.

We believe that this project has only scratched the surface of what is possible in the RAFT synthesis of polymeric SNAP-tag labels. Introduction of the O^6-benzylguanine moiety is the biggest synthetic challenge in the development of SNAP-tag labels, and we have developed a facile method by which to achieve this.

5.3. References

(1) Keppler, A.; Gendreizig, S.; Gronemeyer, T.; Pick, H.; Vogel, H.; Johnsson, K. *Nat. Biotechnol.* **2002**, *21* (1), 86–89.

(2) Torchilin, V. P.; Trubetskoy, V. S.; Narula, J.; Khaw, B. A.; Klibanov, A. L.; Slinkin, M. A. *J. Control. Release* **1993**, *24* (1–3), 111–118.

(3) Lou, X.; Zhang, G.; Herrera, I.; Kinach, R.; Ornatsky, O.; Baranov, V.; Nitz, M.; Winnik, M. A. *Angew. Chem. Int. Ed.* **2007**, *46* (32), 6111–6114.

(4) Majonis, D.; Herrera, I.; Ornatsky, O.; Schulze, M.; Lou, X.; Soleimani, M.; Nitz, M.; Winnik, M. A. *Anal. Chem.* **2010**, *82* (21), 8961–8969.